

Online battery state-of-charge estimation methods in micro-grid systems

Sofia Boulmrharj^{a,b,*}, Radouane Ouladsine^a, Youssef NaitMalek^{a,c}, Mohamed Bakhouya^a, Khalid Zine-dine^d, Mohammed Khaidar^b, Mustapha Siniti^b



^a College of engineering and architecture, LERMA Lab, International University of Rabat, Sala El Jadida 11100, Morocco

^b CUR"EnR&SIE", Faculty of Sciences El Jadida - Chouaib Doukkali University, El Jadida 24000, Morocco

^c ENSIAS, Mohamed V University, Rabat 10000, Morocco

^d Mohammed V University, Faculty of Science, Rabat 10000, Morocco

ARTICLE INFO

Keywords:

Battery characterization
Parameters identification
Battery modeling
Online SOC estimation
MG systems
Performance assessment

ABSTRACT

Batteries have shown great potential for being integrated in Micro-Grid (MG) systems. However, their integration is not a trivial task and, therefore, requires extensive modeling and simulations in order to efficiently estimating their State-of-Charge (SoC) within MG systems. The work presented in this article focuses mainly on battery modeling for SoC estimation. We put more emphasize on battery system's characterization, modeling, SoC estimation and its integration into MG systems in order to study its performance. In fact, an instrumentation platform, composed of recent and low cost sensing and actuating equipment, is developed in order to identify the battery's parameters and then build the battery model. The simulation results show good agreement with the experimental results, and thus the battery model is validated in both charging and discharging processes. Then, the battery's SoC estimation in both charging and discharging processes is investigated by means of sophisticated methods, such as, Artificial Neural Network, Luenberger observer and Kalman Filter combined with Coulomb counting. The results of these methods are reported and compared to the SoC estimated using the Coulomb counting method in order to end up with the precise method. The modeled battery is afterwards integrated into an MG system, which is deployed into our EEBLab (Energy Efficient Building Laboratory) test-site, for simulation and experimental investigations. Finally, the four algorithms for SoC estimation are included into the instrumentation platform, which is connected to a Lead-acid battery already integrated into the MG system, in order to show and compare their performances and accuracy for online battery's SoC estimation.

1. Introduction

The strong emergence of Micro-Grid (MG) systems has appealed much interest to the energy storage systems (e.g., batteries, Pumped Hydroelectric Energy Storage (PHES), flywheels, superconductor, molten salt, hydrogen) [1–3] because of the intermittent nature and the production uncertainty of Renewable Energy Sources (RES). The main purpose is to store the overproduction of RES systems that will be used when there is no production. In fact, the important advantages of batteries (e.g., fast response, modularity, and good energy efficiency) make them among the most used storage devices in MG systems [2]. As a matter of fact, various types of batteries exist, such as, Lead-acid batteries, Lithium ion batteries, Sodium Sulfur batteries, Nickel Cadmium batteries to name a few [1,2].

Battery modeling and performance assessment is, however, necessary for assessing their behavior, especially in MG systems, using both experiments and simulations. Actually, several battery models have

been developed by the research community, such as, the electrochemical models and the electrical-circuit models, in order to estimate, predict and analyze their behavior under different conditions (e.g., charging/discharging current, temperature) [4–6]. The electrochemical models are the most accurate; however, the complex electrochemistry of batteries as well as their temperature reliance makes these models too complex for presenting the batteries' dynamics for the aim of estimating their SoC and identifying their parameters [7]. A simpler alternative to these models are the electrical-circuit models (e.g., ideal battery models, Thevenin battery models), which are widely used in order to estimate, in analogy with electricity, the dynamic batteries' behavior [8]. They are the most used, especially when the battery model is integrated into MG systems, and this is attributed to the fact that they could maintain an acceptable computation complexity while providing a suitable accuracy [5]. These models, which are composed of a voltage source, resistors and capacitors, are increasingly more accurate when the order of the model increases (i.e., RC networks) [9].

* Corresponding author at: College of engineering and architecture, LERMA Lab, International University of Rabat, Sala El Jadida 11100, Morocco.

E-mail address: boulmrharj@gmail.com (S. Boulmrharj).

However, the identification of the battery's parameters, which their number depends on the used model, is required in order to get an accurate battery model that simulate the real battery's behaviour. In fact, several algorithms (e.g., Recursive Least Squares, Neural Networks, Kalman Filter) and experimental tests, such as, OCV tests, impedance spectroscopy, and Hybrid Pulse Power Characterization (HPPC) test, have been proposed and developed in order to accurately identify the batteries' parameters [10–14].

Furthermore, the battery's State of Charge (SoC) is an important indicator for determining the battery's remaining capacity in order to protect it against the deep discharge and the overcharge, which are mainly responsible for the reduction of the battery's lifetime. However, this indicator cannot be measured directly by sensors leading to the necessity of its estimation with mathematical methods. Thus, several methods and algorithms have been proposed and reported in the literature for accurate estimation of the battery's SoC, such as the direct measurement methods, the artificial intelligence methods, the model-based methods, and the hybrid methods [15–20]. Actually, the direct measurement methods (e.g., coulomb counting method, electrochemical impedance spectroscopy method, Open Circuit Voltage (OCV) method) use the dynamic measurement of the battery characteristics in order to estimate the battery's SoC [21]. However, they are less accurate because of the measurement noises and the inaccurate initial value of the battery's SoC. On the other hand, the artificial intelligence methods, such as the Neural Network and the Fuzzy logic, and the model-based methods (e.g., Luenberger observer, Sliding mode observer, Kalman filter) are the most used for estimating the battery's SoC with more precision and accuracy [22–24]. Regarding the hybrid methods, their main purpose is to make the best use of the advantages of each method and thus improving the accuracy and the efficiency of the battery's SoC estimation [25]. Although, the strong dependency on charging/discharging cycle's parameters (e.g., voltage, current, temperature) makes the estimation and the prediction of the battery's SoC much more difficult.

The work presented in this article is a part of an ongoing project that aims to deploy an MG system for simulation and experimental purposes, especially dimensioning and control approaches [26–30]. The MG system is composed of six main components, PV panels in order to generate electricity from solar radiation, Wind Turbines (WT) in order to produce electricity from the wind, batteries that are used as an energy storage system to operate the appliances when there is no production, regulator to control the batteries' charging and discharging processes, inverter to convert the Direct Current (DC) into an Alternating Current (AC), and finally the electric grid that aims at supplying electricity to the buildings' appliances when there is no production and the batteries are empty. In [5,26–30], authors have already developed and validated the models of the main components of the MG system, such as PV panel, wind turbine, regulator, battery, AC/DC converter, DC/AC converter and the electric grid. In this paper, we want to focus especially on the online battery's SoC estimation in MG systems. In fact, several works have studied the SoC estimation of isolated batteries by means of many methods and algorithms [31], while few other works have investigated the batteries' SoC estimation in MG systems for control purposes [32–37].

For instance, authors in [31] have compared the performances of two nonlinear Kalman Filters for online SoC estimation of isolated batteries. Besides, Belvedere et al. [32] have used a combination of the coulomb counting, the OCV and the model-based methods for online battery's SoC estimation. This latter has been used as input to a proposed control approach for MG systems. Also, Blaif et al. [33] have used the coulomb counting method for an online SoC estimation of a battery integrated into an MG system. The data acquisition has been conducted using a National Instruments (NI) microcontroller, and the simulation has been carried out by means of Labview software. Moreover, Arcos-Aviles et al. [34] have investigated an online SoC estimation based on the battery power. The estimated SoC has been used as input to a Fuzzy

Logic control for MG systems. The data acquisition has been performed using an NI instrument, and the control algorithm as well as the SoC estimation have been conducted using the Labview software. Additionally, Cheddadi et al. [35] have investigated the SoC estimation using the coulomb counting method in order to control an MG system. A microcontroller is used for data acquisition, and then the data is transmitted to a host computer, which uses Labview software for control purposes. Furthermore, a comparison between the OCV, coulomb counting and neural network methods, which represents two different categories of SoC estimation methods (direct measurement methods and artificial intelligence methods), for online SoC estimation in MG systems has been investigated [36]. In fact, a data acquisition card is used to measure the battery's parameters, which are then send to a computer where the SoC estimation is performed. Finally, Berrueta et al. [37] have used the coulomb counting, the electrical model circuit and the observer methods, which represents two different categories of SoC estimation methods (direct measurement methods and model-based methods), for SoC estimation in MG systems. The three methods have been compared in terms of accuracy and robustness to current measurement offset and battery aging.

Therefore, in the best of our knowledge, none have compared the accuracy of the four different categories of SoC estimation for an online battery's SoC estimation in MG systems including their implementation in real-sitting scenarios. Thus, the main contributions of this work are as follows: i) an instrumentation platform, composed of recent and low cost sensing and actuating equipment, has been developed and deployed in order to identify the battery's parameters, ii) the battery model has been built and validated in both charging and discharging processes, iii) the battery's SoC estimation in both charging and discharging processes has been investigated by means of sophisticated methods, such as Artificial Neural Network, Luenberger observer and Kalman Filter combined with Coulomb counting, iv) the performance of these methods has been compared to the SoC estimated using the Coulomb counting method in order to end up with the precise method, v) the integration of the modeled battery into an MG system, which is composed of PV panels, converters, batteries and the electric grid, and deployed into our EEBLab (Energy Efficient Building Laboratory) test-site, for simulation and experimental investigations, and finally vi) the four mature algorithms for SoC estimation have been included into the instrumentation platform, which is connected to a Lead-acid battery already integrated into the MG system, in order to show and compare their performances and accuracy for online battery's SoC estimation.

The current article gives in Section 2 an overview of the existing battery models in the literature. Section 3 provides an overview of the methods used for battery parameters identification noting the used one. Then, an overview of the developed methods and algorithms for battery's SoC estimation is presented in Section 4. Section 5 introduces the simulation and experimental results of battery characterization, modeling and SoC estimation. Finally, Section 6 outlines the main conclusions and perspectives.

2. Battery modeling

Battery modeling is mandatory for estimating and assessing its behavior and dynamical response under different conditions, especially in MG systems, using both experiments and simulations. Thus, an overview of battery models as well as the proposed model is introduced in this section. Actually, numerous battery models have been developed these last decades, such as, the electrochemical models and the electrical-circuit models, in order to estimate, predict and analyze its behavior in real-time and under different conditions (e.g., charging/discharging current) [4–6,38]. In fact, the electrochemical models are the most accurate. However, the complex electrochemistry structure of batteries as well as their temperature reliance makes these models too complex for presenting the batteries' dynamics for the aim of estimating their SoC and identifying their parameters [7]. As alternative models,

those based on mathematical equations or on electrical equivalent circuits are extensively used in order to estimate the dynamic batteries' behaviour since they have some important advantages, such as, simplicity and easy online implementation. In fact, the Electrical-Circuit Models (ECMs), such as, ideal battery models and Thevenin battery models, are a combination of a voltage source, resistors and capacitors that simulate, in analogy with electricity, the battery's dynamic behaviour [8,9]. They are the most used, especially when the battery model is integrated into MG systems, and this is attributed to the fact that they could maintain an acceptable computation complexity while providing a suitable accuracy [5].

The ECMs become increasingly more accurate when the order of the model increases (i.e., RC networks), but also more complicated [39,40]. Moreover, the complexity of the battery parameters identification increases when the number of the RC networks of the model increases (i.e., more parameters to identify) [39]. Actually, one to three RC networks are usually used and are sufficient for any application as presented by authors in [39–41]. Besides, authors in [42] have examined and compared three electrical-circuit battery models (R model, 1RC model, 2RC model) in terms of accuracy and computation time for online applications, where a trade-off between accuracy and complexity has to be established. They found that the R model is the fastest one, but, with less accuracy. Besides, when comparing the 1RC and 2RC models, they found that their identification errors are quite similar; however, the computation time has increased when adding one RC network. Thus, the addition of one RC network has increased the complexity of the model, but provided only a small improvement of its accuracy. Furthermore, twelve equivalent circuit models have been compared by authors in [43] in terms of complexity, accuracy and robustness. The first-order RC model was found to be the one that provides a suitable accuracy and robustness with an acceptable complexity. Therefore, the first-order RC model, which is depicted in Fig. 1, is investigated in our work due to its suitable accuracy, acceptable complexity and easy implementation. In this figure, V_{oc} represents the battery's OCV (Open Circuit Voltage), R_1 being the internal resistance, R_2 stands for the polarization resistance, C_2 being the polarization capacitor, V_{bat} represents the terminal battery voltage and I_{bat} stands for the battery current, which is negative in the discharging mode and positive in the charging mode. From the electrical equivalent circuit of the first order RC model (Fig. 1), Eqs. (1)–(3) could be derived, where v represents the measurement noises, w_1 and w_2 are the model uncertainties, η being the battery's efficiency, and C_N stands for the battery's nominal capacity [22].

$$\frac{dV_{RC}}{dt} = -\frac{V_{RC}}{R_2 C_2} + \frac{I_{bat}}{C_2} + w_1 \quad (1)$$

$$\frac{dSoC}{dt} = \frac{\eta * I_{bat}}{C_N} + w_2 \quad (2)$$

$$V_{bat} = V_{oc}(SoC) + R_1 * I_{bat} + V_{RC} + v \quad (3)$$

Supposing that x , which is represented by $\begin{bmatrix} V_{RC} \\ SoC \end{bmatrix}$, is a state space

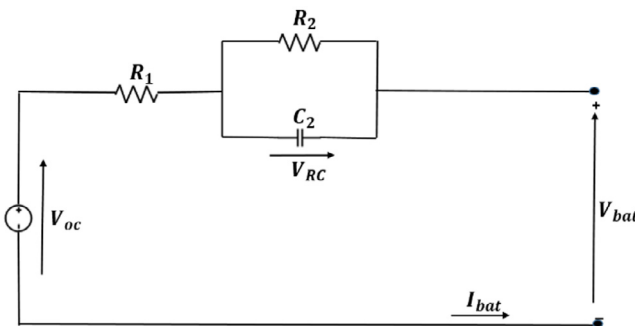


Fig. 1. The electrical equivalent circuit of the first order RC model.

vector, thus Eqs. (1)–(3) could be expressed using Eqs. (4) and (5), where $A = \begin{bmatrix} -1 & 0 \\ R_2 * C_2 & 0 \end{bmatrix}$, $B = \begin{bmatrix} \frac{1}{C_2} \\ \frac{\eta}{C_N} \end{bmatrix}$, $C = [1 \ 0]$, $D = R_1$, $w = \begin{bmatrix} w_1 \\ w_2 \end{bmatrix}$, $u = I_{bat}$, and $y = V_{bat} - V_{oc}$ [22].

$$\frac{dx}{dt} = A*x + B*u + w \quad (4)$$

$$y = C*x + D*u + v \quad (5)$$

The discrete-time state functions, which are obtained using the Euler approximation, could be expressed using Eqs. (6) and (7), where $A_d = I + A*\Delta t$, $B_d = B*\Delta t$, and $w' = w*\Delta t$, with Δt being the sampling time that verifies the Shannon rules, I stands for the Identity matrix, and x_k , x_k' , w_k , y_k , v_k represent the state vectors at time step k [22].

$$x_{k+1} = A_d * x_k + B_d * u_k + w'_k \quad (6)$$

$$y_k = C*x_k + D*u_k + v_k \quad (7)$$

In order to simulate this model, the battery's OCV in Eq. (3) has to be determined. It represents the battery's terminal voltage when there is no load and the battery is at equilibrium and it is highly dependent on the battery's SoC. Several models (e.g., linear, polynomial, exponential, logarithmic, combined model), as reviewed in Fig. 2, have been developed and presented in the literature in order to establish the relationship between the battery's OCV and its SoC [21,44]. For instance, the linear model is the simplest one; however, it doesn't take into consideration the nonlinearity relationship between the two variables. The other models (i.e., polynomial, exponential, logarithmic) are more accurate; however, they are more complex and also hard to be implemented in real-time applications. Furthermore, these individual models could be combined in order to improve their accuracy and get as close as possible to the real relationship between the battery's OCV and SoC [45]. In the literature, the most used model is the polynomial model, with an order that could reaches nine, and this is attributed to the fact that it could maintain an acceptable computation complexity while providing a suitable accuracy [45].

In order to present the OCV-SoC curve and identify the relationship between these parameters, we have deployed a platform composed of a battery, current and voltage sensors and electronic cards into our EEBLab, and then an intermittent charge test was carried out. In this experiment, the hysteresis phenomenon was neglected. Therefore, the battery's OCV is computed in each 10% of the battery's SoC during the charge mode, and thus the battery is charged with C/10 current pulses until the SoC reaches 100%. Using the battery's capacity (24 Ah) and the charging current (C/10), the required charging time for increasing the SoC by 10% is 1 h. Besides, the battery must be left in the open circuit for 1 h to achieve the equilibrium voltage in order to get an accurate battery's OCV (Fig. 3(a)). Finally, once the battery is disconnected, the relationship between the OCV and the SoC is obtained, as illustrated in Fig. 3(b).

Based on the measured data, a seventh-order polynomial model is selected to identify the OCV-SoC relationship. Then, its parameters are obtained using the parameter estimation tool implemented in Matlab/Simulink, which is based on the Recursive Least Squares algorithm [46]. The obtained mathematical expression of the OCV-SoC curve is expressed using Eq. (8).

$$\begin{aligned} OCV = & (4.3 * 10^{-12} * SoC^7) - (1.8 * 10^{-9} * SoC^6) + (3.09 * 10^{-7} * SoC^5) \\ & - (2.67 * 10^{-5} * SoC^4) + (0.001 * SoC^3) - (0.029 * SoC^2) + (0.39 * SoC) \\ & + 6.79 \end{aligned} \quad (8)$$

On the other hand, an identification of the battery's parameters is required in order to simulate the behavior of the battery and estimate its SoC. Therefore, an overview of the methods used for identifying the battery's parameters as well as the proposed method is introduced in the next section.

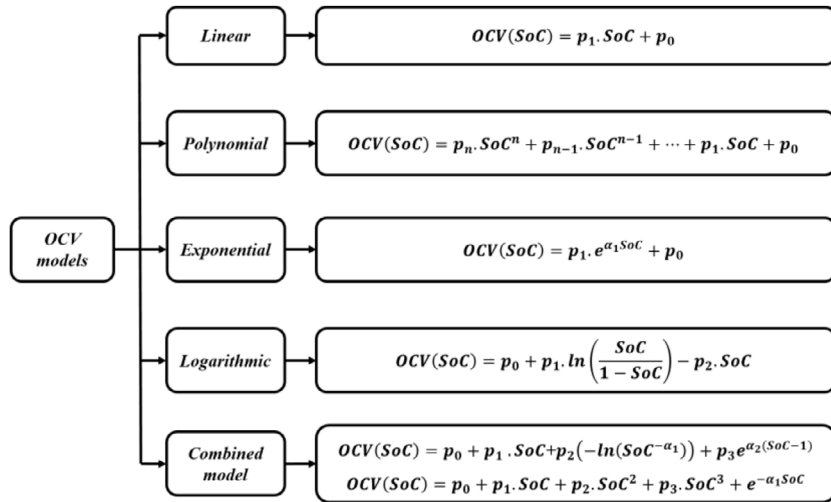


Fig. 2. Overview of the OCV models.

3. Battery parameters identification

The identification of the battery's parameters, which their number depends on the used model, is highly required in order to get an accurate battery model. In the case of the electrical equivalent circuit models, or especially the first order RC model that we have used in this article, three parameters (R_1 , R_2 , C_2) have to be identified. In fact, several algorithms and experimental tests, which are presented in Fig. 4, have been introduced and developed in order to accurately identify these parameters [10–14].

For example, the battery's parameters could be computed by applying current pulses upon successive discharges of the battery, as presented in [23,47]. Another method, called impedance spectroscopy, has been presented by authors in [11]. It is an accurate method; however, it requires specific equipment, which makes it a slightly complicated technique and difficult to be implemented in real-time applications [48]. Furthermore, there is a simpler method that uses three points of the manufacturer's discharge curve for extracting battery parameters, and which is used especially with Shepherd and Tremblay battery models [9]. On the other hand, the battery parameters change with some factors, such as, the depth of discharge, the battery's temperature, and the operating current. Therefore, fixed battery parameters, as the one calculated by the above-mentioned methods, could lead to a significant model error, which reduces the SoC estimation

accuracy. Alternative methods have been then developed in order to identify the battery's parameters in real time. For instance, the Recursive Least Squares (RLS) method (e.g., Levenberg-Marquardt algorithm, Gaussian algorithm, Forgetting Factor algorithm, Trust-region-reflective algorithm) [10], has been used for online battery parameters identification [13,14,22]. The Neural Networks algorithms are also used to identify the battery's parameters even if they are more complex and difficult to be implemented in real-time applications [13]. Moreover, an adaptive Kalman Filter method, called Dual Kalman Filter, has been used by authors in [12,49] for accurately estimating the battery's parameters as well as the SOC estimation. Moreover, authors in [13,38] have computed the battery parameters using the Hybrid Pulse Power Characterization (HPPC) test.

Therefore, an online and accurate identification of the battery's parameters using the RLS method, which is based on experimental data, is presented in this article. The main aim of this method is to find the accurate battery's parameters by minimizing the sum of squares of the residuals, which are the difference between the estimated and measured battery's voltage, in order to best fit the experimental and the simulation results. Thus, the transfer function of the used battery model can be expressed by Eq. (9), with $V = V_{bat} - V_{oc}$ [22].

$$H(s) = \frac{V(s)}{I_{bat}(s)} = \frac{R_2}{1 + R_2 C_2 s} + R_1 \quad (9)$$

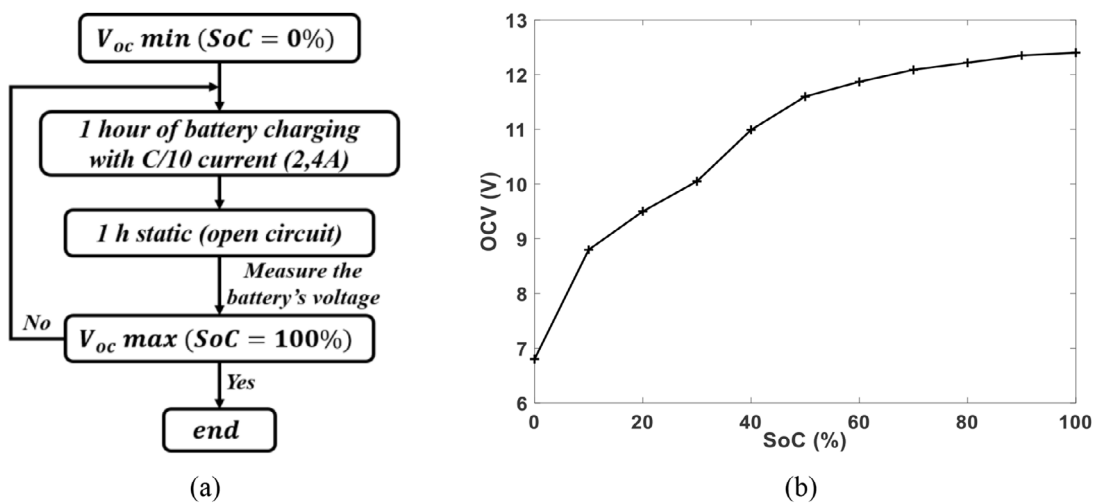


Fig. 3. (a) OCV test, and (b) Experimental OCV-SoC curve.

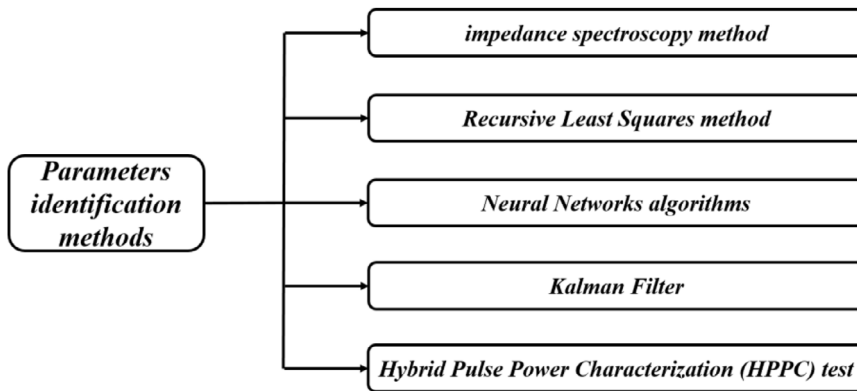


Fig. 4. Battery's parameters identification methods.

Using the bilinear transform rule (i.e., $s = \frac{2*(1-z^{-1})}{\Delta t*(1+z^{-1})}$), the discrete-time form of this transfer function can be rewritten using Eq. (10). Besides, the sampling time Δt , which respects the Shannon rules, is selected to be one second [22].

$$H(z^{-1}) = \frac{V(z^{-1})}{I_{bat}(z^{-1})} = \frac{T_1 + T_2 * z^{-1}}{1 + T_3 * z^{-1}} \quad (10)$$

where:

$$T_1 = \frac{R_1 + R_2 + 2R_1R_2C_2}{1 + 2R_2C_2} \quad (11)$$

$$T_2 = \frac{R_1 + R_2 - 2R_1R_2C_2}{1 + 2R_2C_2} \quad (12)$$

$$T_3 = \frac{1 - 2R_2C_2}{1 + 2R_2C_2} \quad (13)$$

Eq. (10) can be transformed into a time-domain difference equation as expressed in Eq. (14) [22].

$$V_{bat}(k) - V_{oc}(k) = -T_3*(V_{bat}(k-1) - V_{oc}(k-1)) + T_1*I_{bat}(k) + T_2*I_{bat}(k-1) \quad (14)$$

Eq. (14) could be rewritten as Eq. (15) [22].

$$y(k) = T(k)*\emptyset(k)^T \quad (15)$$

where:

$$T(k) = [T_1 \ T_2 \ T_3] \quad (16)$$

$$\emptyset(k) = [I_{bat}(k) \ I_{bat}(k-1) \ -(V_{bat}(k-1) - V_{oc}(k-1))] \quad (17)$$

$$y(k) = V_{bat}(k) - V_{oc}(k) \quad (18)$$

The vector $T(k)$ could be found using the RLS Algorithm with Forgetting Factor λ (equal 1 in this case). This algorithm is established using Eqs. (19)–(22), where $e(k)$ being the estimation error, $G(k)$ stands for the algorithm gain, and $P(k)$ represents the covariance matrix [22].

$$e(k) = y_{measured}(k) - T(k-1)*\emptyset(k)^T \quad (19)$$

$$G(k) = \frac{P(k)*\emptyset(k)^T}{\lambda + \emptyset(k)^T P(k-1) * \emptyset(k)} \quad (20)$$

$$P(k) = \frac{1}{\lambda} * [P(k-1) - G(k)*\emptyset(k)^T P(k-1)] \quad (21)$$

$$T(k) = T(k-1) + G(k)^T e(k) \quad (22)$$

Finally, the battery's parameters, which are R_1 , R_2 and C_2 , could be calculated using the expression of T_1 , T_2 and T_3 as expressed by Eqs. (23)–(25) respectively [22].

$$R_1 = \frac{T_1 - T_2}{1 - T_3} \quad (23)$$

$$R_2 = \frac{2*(T_2 - T_3*T_1)}{1 - T_3^2} \quad (24)$$

$$C_2 = \frac{(1 - T_3)^2}{4*(T_2 - T_3*T_1)} \quad (25)$$

4. An overview of battery's SoC estimation methods

The estimation of the battery's SoC is highly required in order to have an idea about the amount of the remaining energy. Therefore, an overview of the models used in order to estimate this important indicator is introduced in this section. According to [15], the battery's SoC is the ratio between the remaining capacity in the battery (C_t) and the nominal capacity (C_N).

$$SoC = \frac{C_t}{C_N} \quad (26)$$

As mentioned previously, the battery's SoC depends on the variation of many parameters involved in the charge and discharge cycles (e.g., voltage, current, temperature), which makes its estimation much more complicated. Thus, Fig. 5 presents an overview of the methods and algorithms proposed and developed in the literature for estimating the battery's SoC [15–20,50–53]. The detail of each method is given in the next sub-sections.

4.1. Direct methods

Based on the dynamic measurement of different battery parameters, such as, current, voltage and impedance, the direct methods for SoC estimation can be classified into three categories: the Coulomb Counting method, the Open Circuit Voltage (OCV) method and the Electrochemical Impedance Spectroscopy (EIS) method [15,44]. For instance, the Coulomb counting, called also Ah method, is based on the integration of the battery's current over time in order to calculate the remaining battery's capacity, as expressed by Eq. (27), where SoC_{t-1} represents the battery's SoC at time $t-1$, C_N being the battery's nominal capacity (i.e., the capacity given by the manufacturer), η stands for the battery's efficiency, which is close to 1 under room temperature, I_{bat} represents the battery's current, and t is the sample time [15,44].

$$SoC_t = SoC_{t-1} + \left(\frac{1}{C_N} \right) \int_{t-1}^t \eta I_{bat} dt \quad (27)$$

The Ah method is the most used technique for battery's SoC estimation due to its easy implementation. Nevertheless, because of the cumulative errors in current measurement due to the noises and the

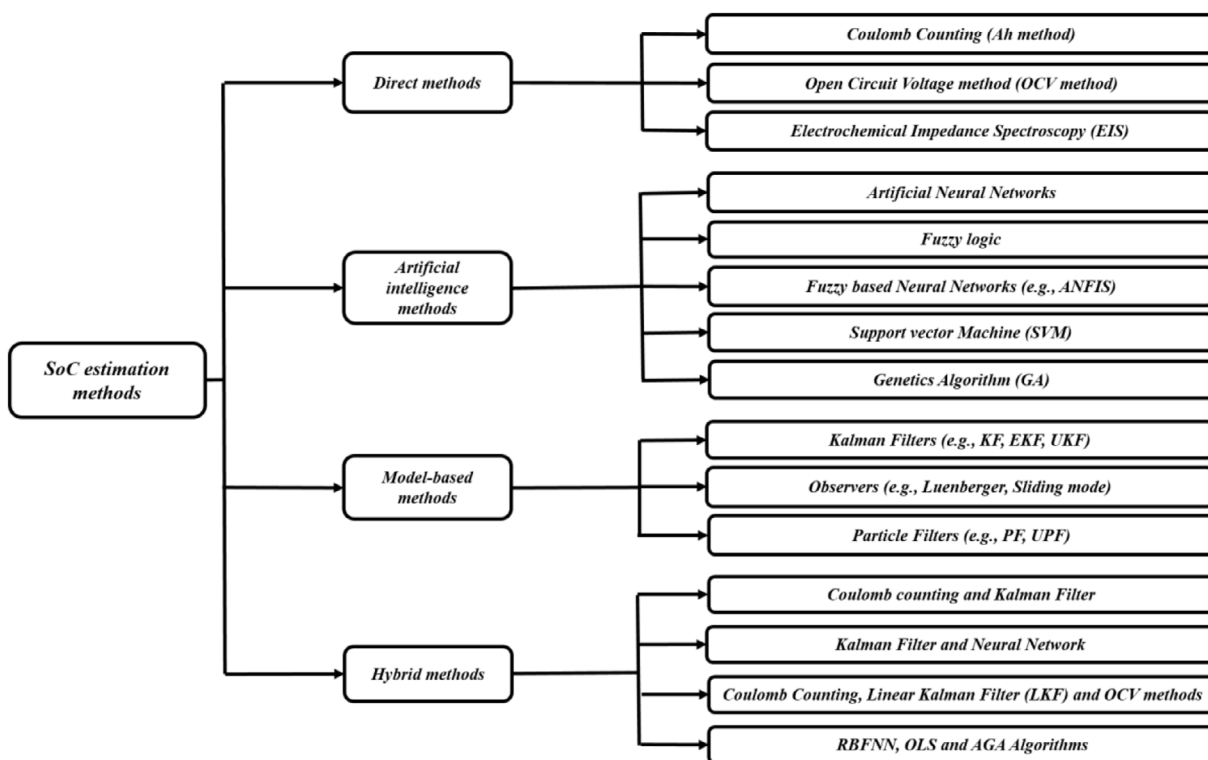


Fig. 5. SoC estimation methods.

inaccurate initial value of the battery's SoC, the estimated SoC contains considerable errors [44]. On the other hand, the OCV method aims at establishing a relationship between the battery's OCV and SoC. However, the battery takes too much time to reach the stable state, which makes this method too much difficult to be implemented in practice [15,44]. Finally, the EIS, which is an accurate method, uses the battery's impedance as an input in order to estimate its SoC [11,15]. However, the specific equipment required by this method makes it impractical and difficult to implement in real-time applications [15,48].

4.2. Artificial intelligence methods

The artificial intelligence methods, such as, Artificial Neural Network and Fuzzy Logic, are widely used for estimating the battery's SoC due to their high accuracy [15,24,44,54–56]. The learning capability of these methods makes them able of adjusting the battery model by minimizing the error, which is the difference between the simulated result and the actual measurement, in order to provide an accurate battery's SoC. For instance, authors in [24] have used the Artificial Neural Network in order to estimate the battery's SoC using the recent history of battery's voltage and current. Besides, authors in [56] have used the learning capabilities of the Fuzzy Logic in order to accurately estimate and predict the battery's SoC. Furthermore, several approaches that combine the Neural Network and the Fuzzy Logic algorithms have been presented in [57]. However, these methods are complex to be implemented in practice. Other methods, such as the Support Vector Machine (SVM) and the Genetic Algorithm (GA), have been also used these last decades in order to precisely estimate the battery's SoC [15,16].

Regarding the Artificial Neural Network (ANN), which is used in this work in order to accurately estimate the battery's SoC, it is a model based on recent history and data of the battery and it is widely used to model non-linear systems, such as, the battery's SoC and State of Health (SoH) [56,58]. It is constituted of neurons, as it is depicted in Fig. 6, which are connected in order to develop a relationship between the

ANN's inputs and outputs [56].

This model is expressed, in our case, by Eq. (28), where SoC_{k-1} , I_k , and I_{k-1} represents the inputs of the neuron, a_1 , a_2 , and a_3 being their weights respectively, $F(AX)$ stands for the activation function, and b being the bias [56].

$$SoC_k = F(AX) = F(a_1 SoC_{k-1} + a_2 I_k + a_3 I_{k-1} + b) \quad (28)$$

The activation function could be either a linear function or a sigmoid or any other function [56]. Then, this algorithm has been implemented in Matlab. It has been used in order to identify the different coefficients (i.e., weights) using a recent history of the battery parameters. Once the weights have been identified, the algorithm has been used in order to estimate the battery's SoC in real time.

4.3. Model-based methods

Luenberger observer, Sliding mode observer, Kalman filter, Proportional integral observer (PIO), Particle Filter (PF), and Moving Horizon Estimation (MHE) are some model-based methods that have been widely studied for accurately estimating the battery's SoC [15,16,18–20,49,59]. These methods have multiple advantages, such as, self-correction, online computation, and dynamic SoC estimation. As depicted in Fig. 7, the model-based methods compute the difference between the simulated and the measured voltage (i.e., the system's error) in order to feed it back, through the model gain, into the battery model for the purpose of adjusting the estimated system states and minimizing the error as well. This closed-loop system seeks to be as accurate as possible in order to precisely estimating the battery's SoC, which depends strongly on the battery model's precision [22,44].

4.3.1. SoC estimation based on Kalman filter

The Kalman Filter (KF), the Extended Kalman Filter (EKF), the Unscented Kalman Filter (UKF), and the Sigma Point Kalman Filter (SPKF) are examples of algorithms that have been proposed and developed as sophisticated methods for estimating the battery's SoC in real time [18,19,22,23,44,47,49,51]. For instance, the KF is dedicated

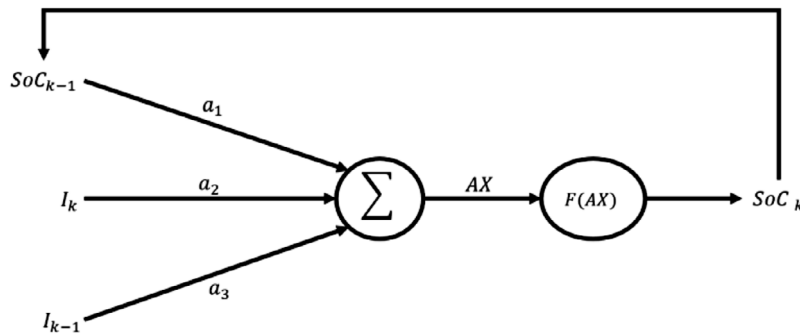


Fig. 6. Artificial Neural Network model.

to estimate the states of linear systems, while the UKF and EKF are developed in order to estimate the states of nonlinear systems [22,23,44,47]. Furthermore, another variety of this method, called Dual EKF, combines two EKF algorithms for concurrently estimating and computing the battery's SoC as well as the battery's parameters [10]. Fig. 8 depicts the process of the KF algorithm for accurately estimating the battery's SoC.

4.3.2. SoC estimation based on Luenberger observer

The Luenberger observer was firstly proposed and designed to be applied to linear systems. Then, it has been extended to nonlinear systems. Therefore, several studies have been conducted in order to design the observer's gain for both linear and non-linear systems. Thus, this observer has been widely used in order to estimate the battery's SoC, even if the battery model is presented by a nonlinear system [44,59]. Its equations are expressed by Eqs. (29) and (30), where L represents the Luenberger gain, which has to be chosen so that $(A - LC)$ is Hurwitz. This error is given by Eq. (31), with $\frac{dx_{\text{measured}}}{dt} = Ax_{\text{measured}} + Bu$.

$$\frac{dx_{\text{estimated}}}{dt} = Ax_{\text{estimated}} + Bu + L(y_{\text{measured}} - y_{\text{estimated}}) \quad (29)$$

$$y_{\text{estimated}} = Cx_{\text{estimated}} + Du \quad (30)$$

$$\begin{aligned} \frac{de(t)}{dt} &= \frac{dy_{\text{measured}}}{dt} - \frac{dy_{\text{estimated}}}{dt} = C\left(\frac{dx_{\text{measured}}}{dt} - \frac{dx_{\text{estimated}}}{dt}\right) \\ &= (A - LC)e(t) \end{aligned} \quad (31)$$

4.3.3. SoC estimation based on the sliding mode observer

The sliding mode observer has been recently proposed in order to accurately estimating the battery's SoC [44]. It uses a non-linear gain feedback for the purpose of fitting exactly the estimated output to the

measured one. Thus, the observer's non-linear gain is established with a switching function (sgn (sgn)) of the difference between the measured and the estimated output. The equations of the sliding mode observer are given by Eqs. (32) and (33), where H represents the gain matrix, ρ being the switching gain, and

$$\text{sgn}(y_{\text{measured}} - y_{\text{estimated}}) = \begin{cases} +1 & \text{when } (y_{\text{measured}} - y_{\text{estimated}}) > 0 \\ -1 & \text{when } (y_{\text{measured}} - y_{\text{estimated}}) < 0 \end{cases}$$

$$\frac{dx_{\text{estimated}}}{dt} = A*x_{\text{estimated}} + B*u + H*(y_{\text{measured}} - y_{\text{estimated}}) + \rho * \text{sgn}(y_{\text{measured}} - y_{\text{estimated}}) \quad (32)$$

$$y_{\text{estimated}} = C*x_{\text{estimated}} + D*u \quad (33)$$

4.4. Hybrid methods

The main purpose of hybrid methods is to make the best use of the advantages of the above-mentioned methods, and thus improving the accuracy of the battery's SoC estimation. Therefore, they aim at estimating a precise and accurate battery's SoC compared to the one estimated by the individual methods. In fact, several hybrid methods for battery's SoC estimation have been proposed by the research community. For instance, the battery's SoC estimation has been performed by mixing the Coulomb-Counting and the model-based estimation approaches, as presented in [60]. The results of this hybrid method have proven its robustness. Also, a combination of the EKF and the Neural Network methods have been proposed in [25], and obtained results showed that this combination gives an accurate battery's SoC. Besides, authors in [40] have presented a hybrid approach that combines three different SoC estimation approaches, which are the Coulomb-Counting, the Linear Kalman Filter (LKF) and the OCV-based methods, in order to provide a more accurate battery's SoC estimation. Moreover, a hybrid method has been proposed in [61] in order to precisely estimate the

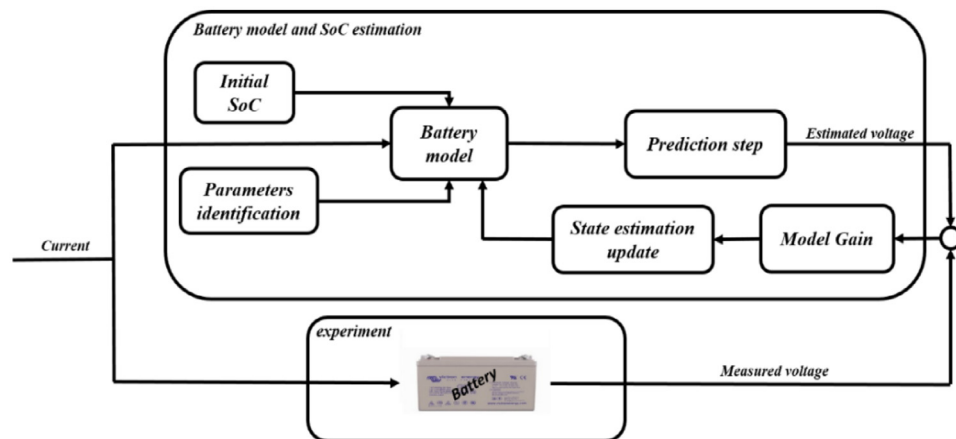


Fig. 7. Equivalent block diagram of the model-based SoC estimation methods.

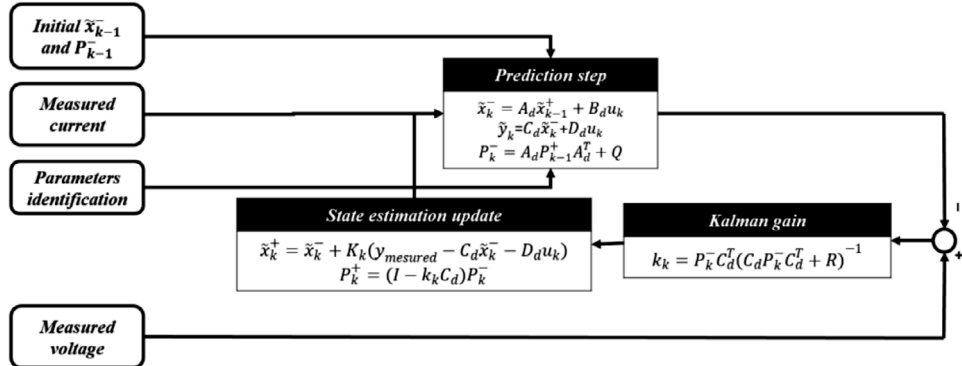


Fig. 8. Recursive KF algorithm.

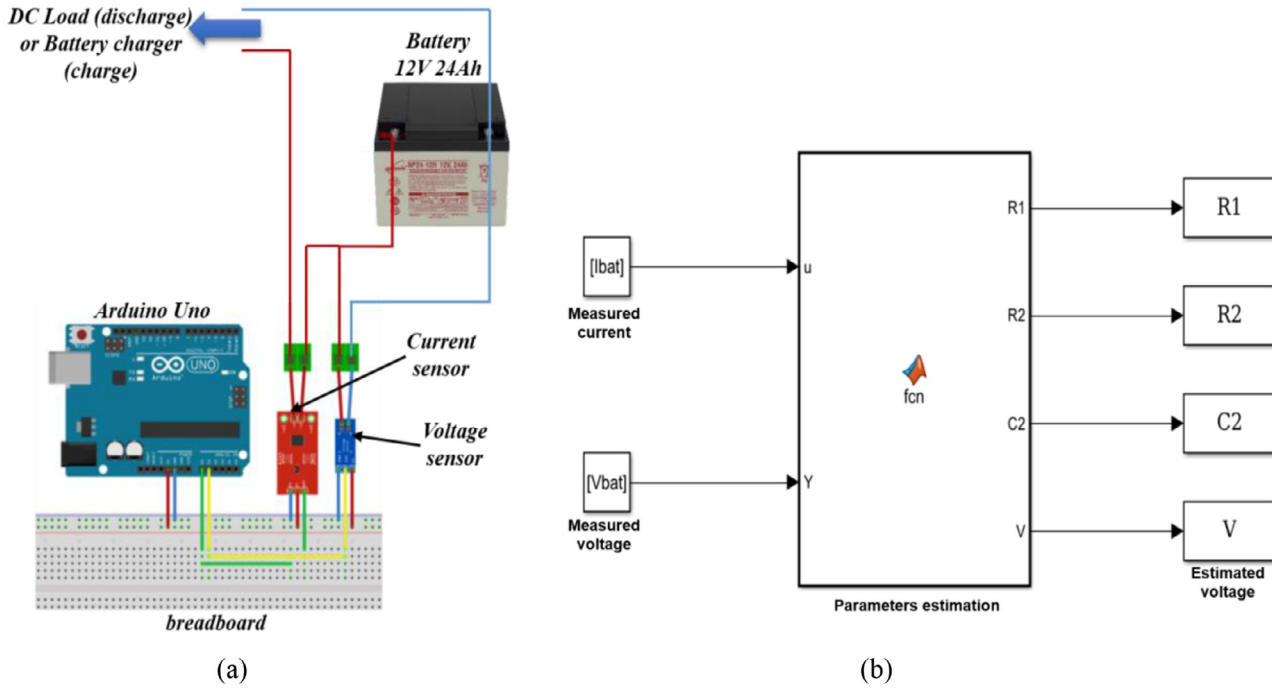


Fig. 9. (a) Instrumentation platform for battery characterization, and (b) the Simulink model of the battery parameters identification.

battery's SoC. The proposed method combines three different methods, a Radial Basis Function (RBF) neural network, an Orthogonal Least-Squares (OLS) algorithm and an Adaptive Genetic Algorithm (AGA). This method has been compared to the Coulomb Counting method and a Back Propagation (BP) neural network, and the results showed that the proposed hybrid method is more accurate than the other methods. Furthermore, in [62], authors have presented a hybrid SoC estimation method, named Kalman-Ah method. It is a combination between the Coulomb Counting and the Kalman Filter methods. In this method, the Kalman Filter is used for correcting the SoC initial value of the Coulomb Counting by converging it to its real value. Then, the SoC is estimated by means of the Coulomb Counting method due to its simplicity. This combination makes this method more simple and accurate.

In our work, we have investigated one method for each category depicted in Fig. 5, Coulomb counting (direct), Artificial Neural Network (artificial intelligence), Luenberger observer (model-based), and Kalman Filter combined with Coulomb counting (hybrid), for SoC estimation and their implementation in the context of MG systems.

5. Simulation and experimental results

This section focuses on simulations and experimentations that we

have conducted for battery characterization, and the comparison of SoC estimation methods. In fact, an instrumentation platform have been first developed and deployed, using recent and low cost sensing and actuating equipment, for battery's parameters identification. Then, the identified parameters are used in order to build the battery model. The simulation and experimental results of both the parameters identification methodology as well as the battery model, in both charging and discharging processes, are reported and compared in order to show the effectiveness of the characterization methodology and validate the battery model as well. Then, a comparison between the four categories of battery's SoC estimation (i.e., coulomb counting, artificial neural network, Luenberger observer, and Kalman filter combined with coulomb counting) in both charging and discharging processes has been performed in order to show the accuracy of these methods and to end up with the precise method (i.e., the one with the minimal error). The modeled battery is afterwards integrated into an MG system, which is deployed into our EEBLab (Energy Efficient Building Laboratory) test-site, for simulation and experimental investigations. Finally, the four algorithms for SoC estimation are included into the instrumentation platform, which is connected to a Lead-acid battery already integrated into the MG system, in order to show and compare their performances and accuracy for online battery's SoC estimation.

5.1. Parameters identification and battery model validation

The identification of the battery's parameters using the RLS method, which aims at an online identification of the battery's parameters by fitting the estimated and the measured battery's voltage, requires experimental data (i.e., the battery's voltage and current). In order to extract this data in both charging and discharging processes, we have deployed an instrumentation platform for battery characterization, as depicted in Fig. 9(a). This platform is composed of a Lead-acid battery, which is manufactured by Genesis NP24-12R, with 12 V as nominal voltage and a nominal capacity of 24Ah, a battery charger, a DC load, a current (ACS712) and voltage (from DCT electronic) sensors, a breadboard, and an Arduino Uno as a data acquisition board. The current and voltage sensors, which have been calibrated using sophisticated meters, are connected to the Arduino Uno in order to measure, extract and collect the battery's data, and then send it to a cluster for processing and storage. Then, a web application has been developed in order to extract and visualize the battery features in real time [26]. The extracted battery features have been afterwards fed to the RLS algorithm, which is presented in Fig. 9(b), for online identification and computation of the battery parameters. The main aim is to come up with the battery parameters that fit as much as possible the simulated voltage to the measured one.

Fig. 10 illustrates the steps that we have followed for identifying the battery features and validating its model. In fact, numerous experiments have been carried out in order to extract and collect the battery's current and voltage in both charge and discharge processes, and then the data has been processed and filtered. We have afterwards applied the RLS method to this data for estimating the battery parameters (i.e., R_1 , R_2 , C_2). Then, the estimated parameters have been fed to the battery model. This latter has been simulated under Matlab, and then the estimated and the experimental voltage have been compared in order to validate the battery model.

Fig. 11 depicts the curves of the battery's current and voltage that have been used in order to identify the battery parameters. In fact, we have applied a current pulses of approximately 7.5 A upon successive discharges. We have presented just a part of the discharge curve (Fig. 11), which we have used for estimating our battery features, since the battery parameters converge from the first iterations and the same features are extracted in both charge and discharge processes.

Once the simulation has been finished and the elements of the vector T have converged, as we observe in Fig. 12, the battery parameters have been computed using Eqs. (23)–(25). We have found that R_1 , R_2 and C_2 are equal to 0.033Ω , 0.066Ω and 1500 F respectively.

Once the battery parameters have been computed, they have been included into the battery model. This latter has been simulated with the identified parameters under Matlab in both charge and discharge processes. The simulation results have been compared to the experimental ones in order to first show the accuracy of the battery characterization methodology and then validate the battery model. The established battery's model will be used for estimating the battery's SoC when it is isolated and when integrated into the MG system. Fig. 13 depicts the battery's current and voltage during the discharging process. As it can be observed, the experimental and simulated battery's voltage have similar behavior and match too well. Besides, Fig. 14 presents the battery's current and voltage during the charging process. From this figure, we notice that the experimental and simulated battery's voltage fit too well. Finally, Fig. 15 illustrates the residuals (i.e., the difference between the measured and estimated battery voltage) in both charging and discharging processes. We notice that the residuals do not exceed the threshold, which is 5% [13], in both charge and discharge processes. This slight error could be provoked by not taking into account the effect of temperature on the battery features in the model. From these results, we deduce that the estimated battery parameters fit as much as possible the simulated battery's voltage to the measured one, which leads us to conclude the efficiency and the accuracy of the battery characterization methodology as well as the validation of the battery model.

5.2. Comparison of battery's SoC estimation methods

In this sub-section, a comparison between the four categories of battery's SoC estimation (i.e., Coulomb Counting (CC), Artificial Neural Network (ANN), Luenberger Observer (LO), and Kalman Filter combined with Coulomb Counting (KFCC)) in both charging and discharging processes has been investigated in order to show and compare their accuracy and to end up with the precise method (i.e., the one with the minimal error). Therefore, the battery test bench, which is presented in Fig. 16, has been established in order to evaluate the performance of the considered methods for SoC estimation. It is composed

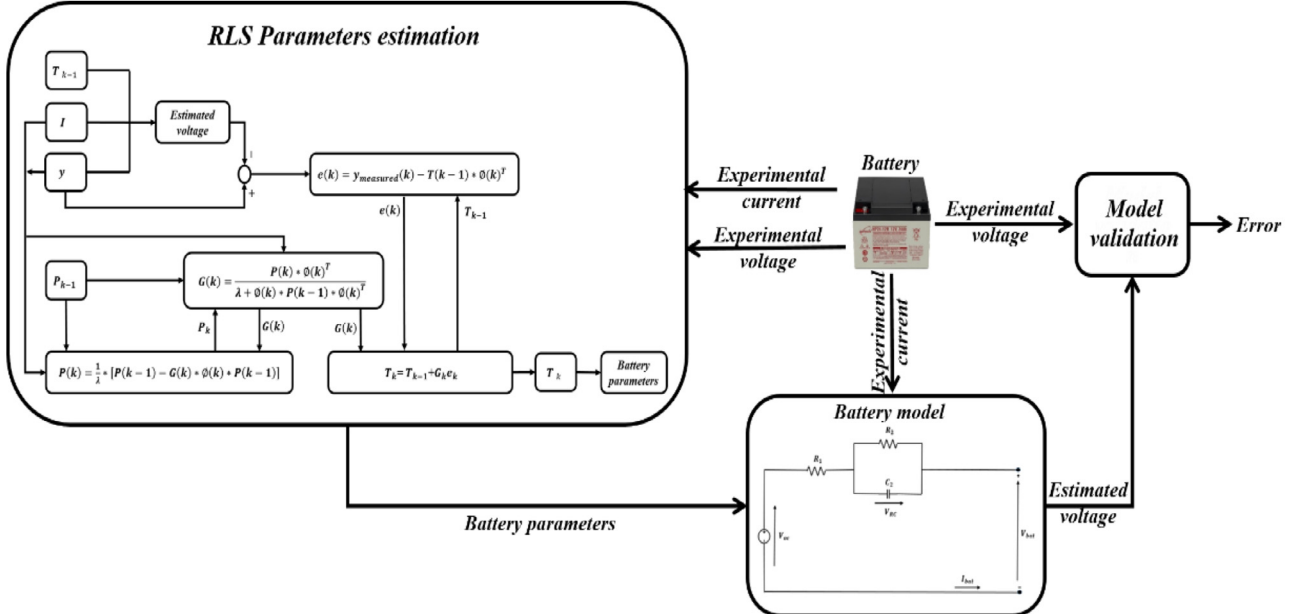


Fig. 10. Block diagram of the battery's parameters identification and model validation.

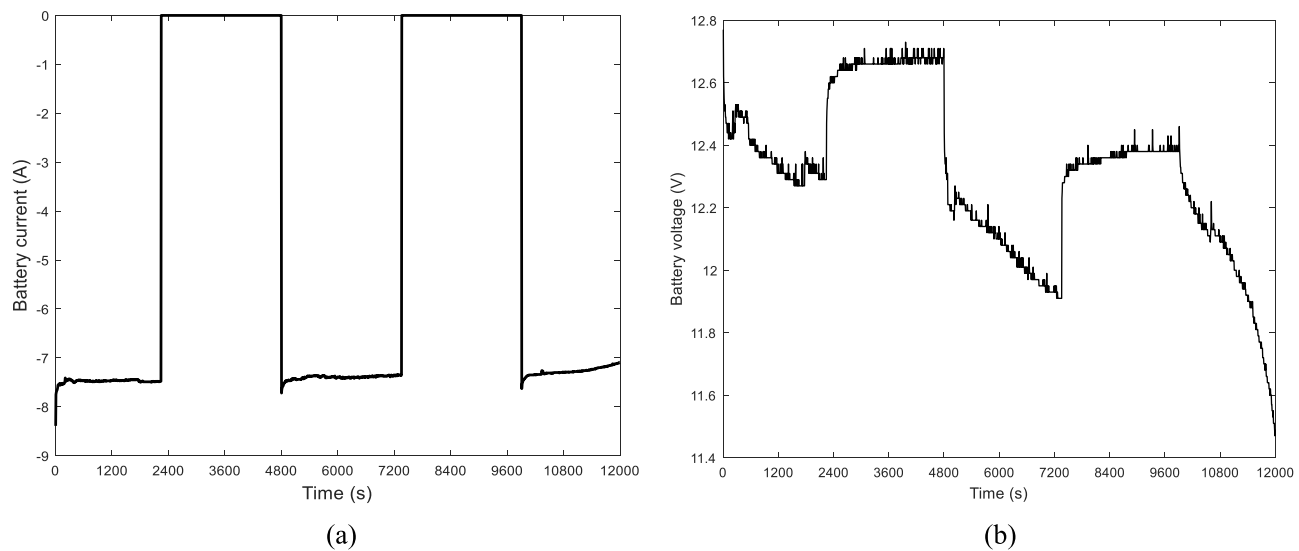


Fig. 11. (a) Discharge current pulses of 7.5A applied to the battery, and (b) Battery's terminal voltage response.

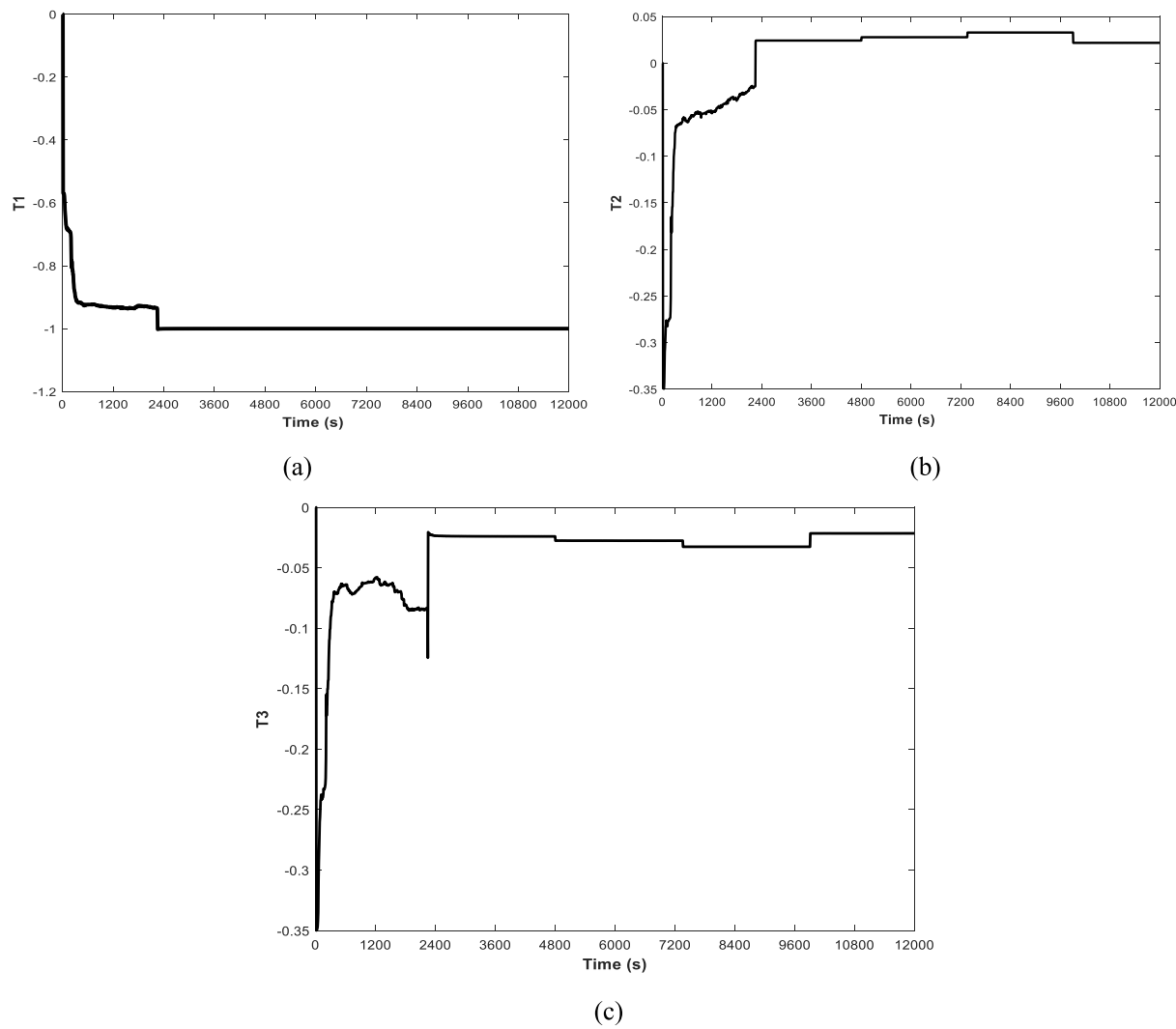


Fig. 12. The evolution and the convergence of the elements of the vector T , (a) T_1 , (b) T_2 , and (c) T_3 .

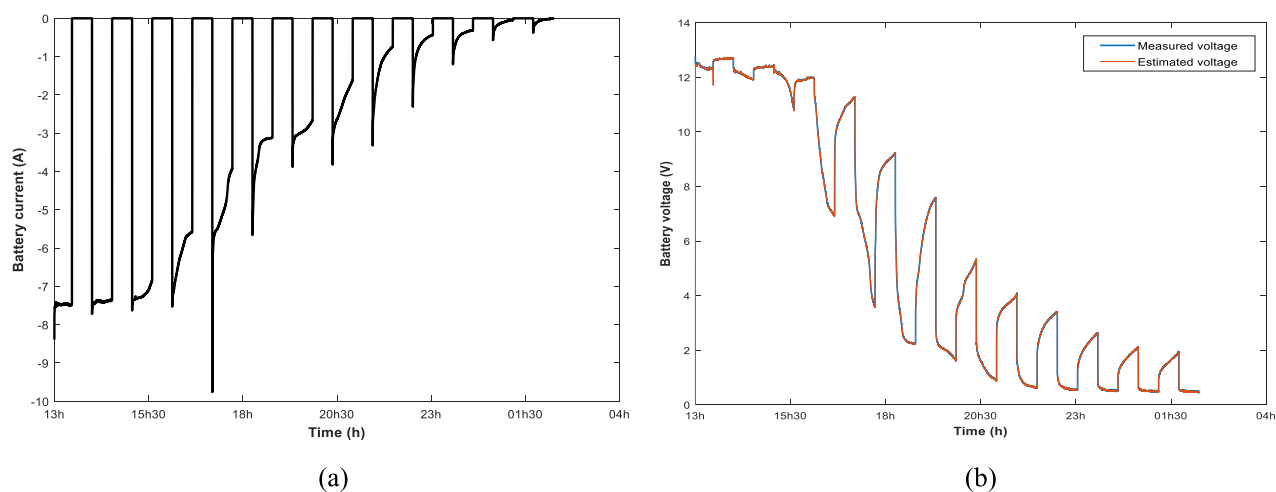


Fig. 13. The battery characteristics during the discharge process (a) Battery's current, and (b) The measured and estimated battery's voltage.

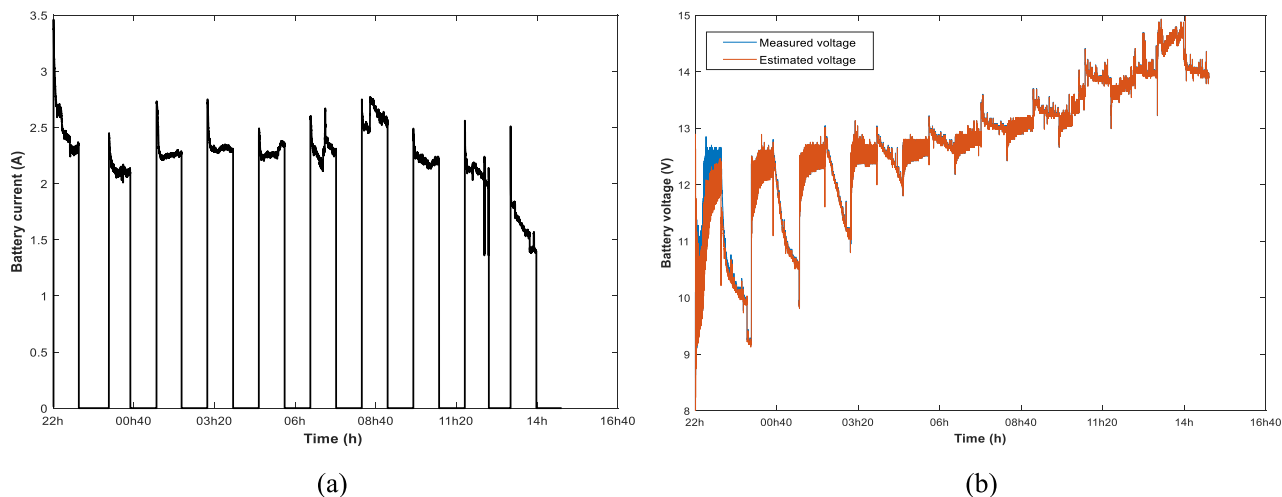


Fig. 14. The battery characteristics during the charge process (a) Battery's current, and (b) The measured and estimated battery's voltage.

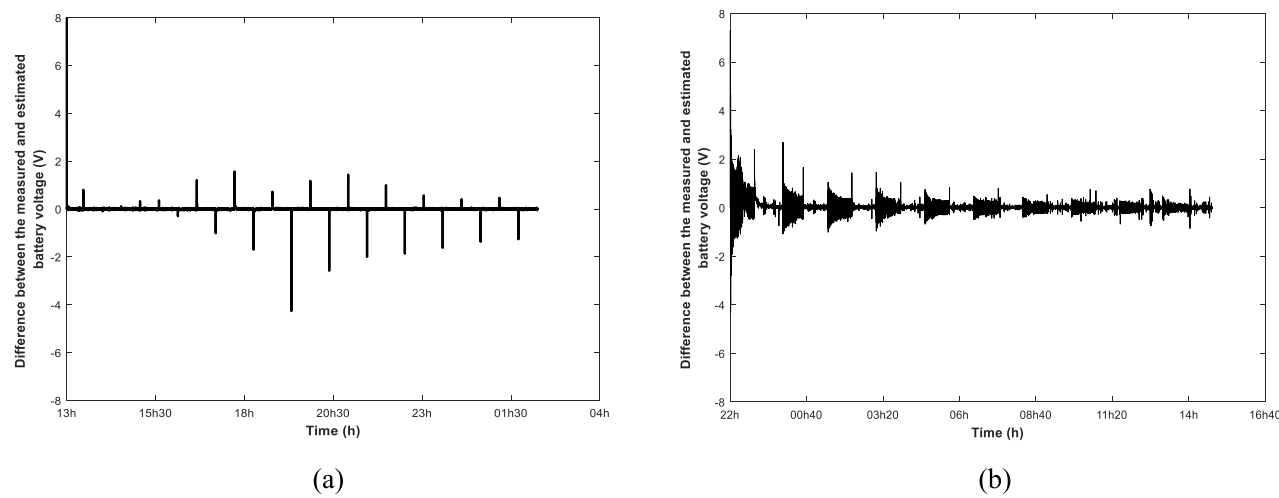


Fig. 15. The residuals in both (a) Discharging process, and (b) Charging process.

of the same instrumentation platform used in the parameters identification (Fig. 9(a)) in order to extract the battery's voltage and current in several charge/discharge cycles, a Raspberry pi, and a computer with Matlab/Simulink software for simulation and comparison purposes.

In fact, the instrumentation platform, especially the Arduino Uno, is

connected to the Raspberry pi using a wire in order to send to it the extracted and collected battery's voltage and current. Then, this data is remotely sent from the Raspberry pi to the computer via Wi-Fi. In the computer, the battery characteristics as well as the validated battery model are used in order to estimate its SoC using the four methods that

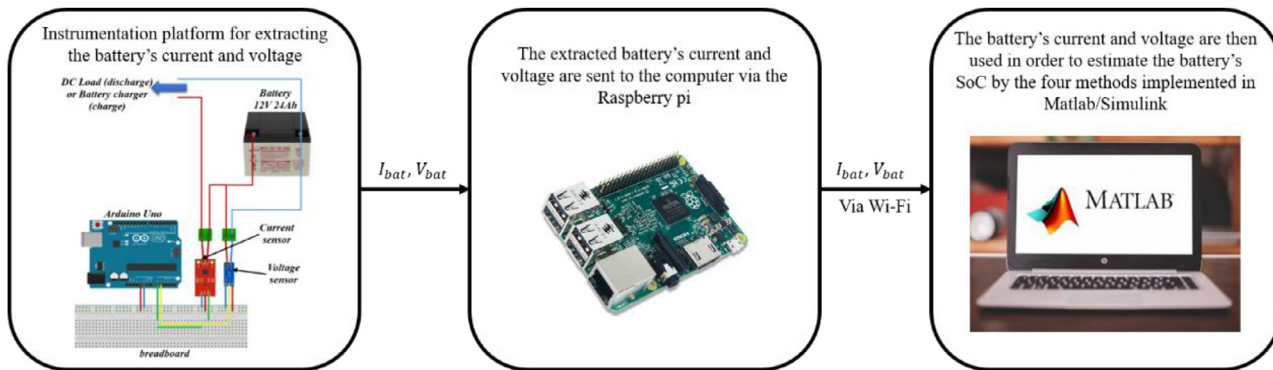


Fig. 16. Block diagram of the battery test bench used for SoC estimation.

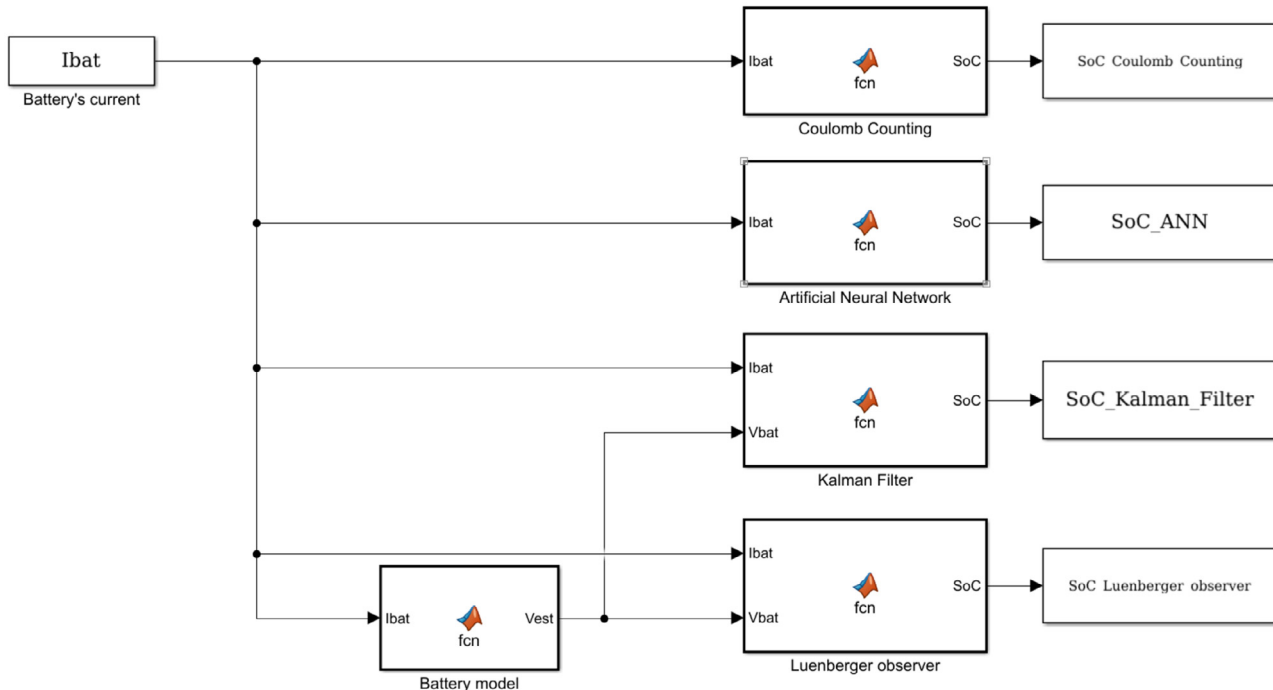


Fig. 17. The Simulink model of the four methods used for battery's SoC estimation.

have been already implemented in Matlab/Simulink, as illustrated in Fig. 17. In our case, we will use the Coulomb Counting method in order to compute the reference SoC in both charging and discharging processes, since we know the battery's initial SoC and the accuracy of the current sensor is sufficient [63,64].

Fig. 18 depicts the estimated battery's SoC by the four methods as well as their error when comparing them to the reference SoC in the discharging process. This estimation was conducted based on measured data, which are the battery's current and voltage presented in Fig. 13. Besides, Fig. 19 depicts the estimated battery's SoC by the four methods as well as their error when comparing them to the reference SoC in the charging process. This estimation was also carried out based on measured data, which are the battery's current and voltage, already illustrated in Fig. 14. We can observe from Figs. 18(a) and 19(a) that the SoC estimated by the ANN, LO, and KFCC have similar behavior as the reference SoC. However, the SoC estimated by the ANN is the closest one to the reference SoC. This can also be seen in Figs. 18(b) and 19(b), where we can observe that the SoC estimated by the ANN has the smallest error compared to the other methods.

Furthermore, Table 1 represents the main indicators, which are the average error, the max error, and the RMSE (Root Mean Square Error), used for showing the difference between the different used algorithms

as well as their accuracy in both charging and discharging processes. The average error and the max error have been computed from the difference between the SoC estimated with the three methods and the reference SoC, which has been calculated at each sampling time. They represent the accuracy of each method to estimate the battery's SoC. On the other hand, the RMSE, which is used to compute the deviation between the estimated and the reference SoC, depicts the stability and the accuracy of the estimated SoC compared to the reference SoC [14]. It is computed using Eq. (34), where $SoC_{estimated}$ represents the SoC estimated using the ANN, KFCC, and LO in each sampling time, $SoC_{reference}$ being the reference SoC in each sampling time, and N stands for the time needed for charging or discharging the battery.

$$RMSE = \sqrt{\frac{1}{N} \sum_{i=1}^N (SoC_{estimated}(i) - SoC_{reference}(i))^2} \quad (34)$$

As we can observe in Table 1, the average error, the max error and the RMSE of the SoC estimated using the ANN method are considerably smaller than those of the SoC estimated using the KFCC and the LO methods in both charging and discharging processes. Hence, the ANN method has higher estimation accuracy compared to the KFCC and LO methods. This can be explained by the fact that the KFCC and LO

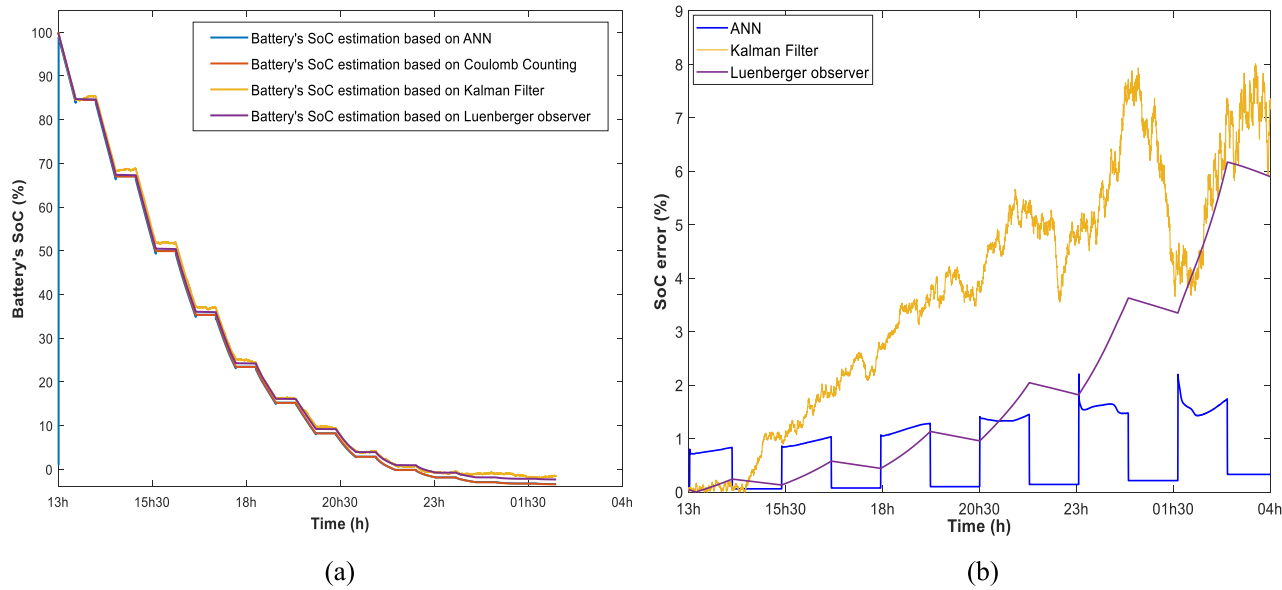


Fig. 18. (a) The battery's SoC, and (b) The SoC estimation error in the discharging process.

methods are based on the battery model as well as its identified parameters. This leads to an accumulation of the errors of the battery model, the battery parameters identification and the SoC estimation, which makes the errors of these two methods higher than the ANN method. On the other hand, ANN uses a learning process, only based on recent history and data of the battery, that is able to estimate and adapt the battery's SoC to the reference SoC, which makes it more accurate.

5.3. Integration and real-testing in MG system

The validated battery model together with the four SoC estimation methods have been integrated into our MG system in both simulation and experimentation in order to show and compare their accuracy for online SoC estimation in MG systems. The proposed MG system, which is depicted in Fig. 20, has been installed in our EEBLab test-site. It is composed of a polycrystalline PV panel manufactured by Amerisolar AS-6P30 with 265 W as rated power (see Table 2 for more features), a regulator fabricated by Victron energy MPPT 75/15, a Lead-acid battery with 12 V as nominal voltage and 24Ah as nominal capacity (the

Table 1

SoC estimation errors of the three methods in both charging and discharging processes.

| Mode | Methods | Average error | Max error | RMSE |
|-----------|---------|---------------|-----------|--------|
| Discharge | ANN | 0.1830 | 0.7782 | 0.2947 |
| | KFCC | 1.3537 | 2.3172 | 1.4457 |
| | LO | 0.8266 | 1.1340 | 0.8918 |
| Charge | ANN | 0.2149 | 0.5492 | 0.3043 |
| | KFCC | 1.5624 | 4.4228 | 1.8352 |
| | LO | 2.3742 | 4.7603 | 2.7509 |

same that we have characterized and modeled), a DC load with 12 V and 24 W as nominal voltage and power respectively, and finally the electric grid in order to supply the load with electricity, through an AC/DC converter, when there is no production and the batteries are empty.

Moreover, a low cost instrumentation platform, composed of current (ACS712) and voltage (from DCT electronic) sensors, actuator (Songle, type SRD-05VDC-SL-C) and Arduino Uno, has been deployed in

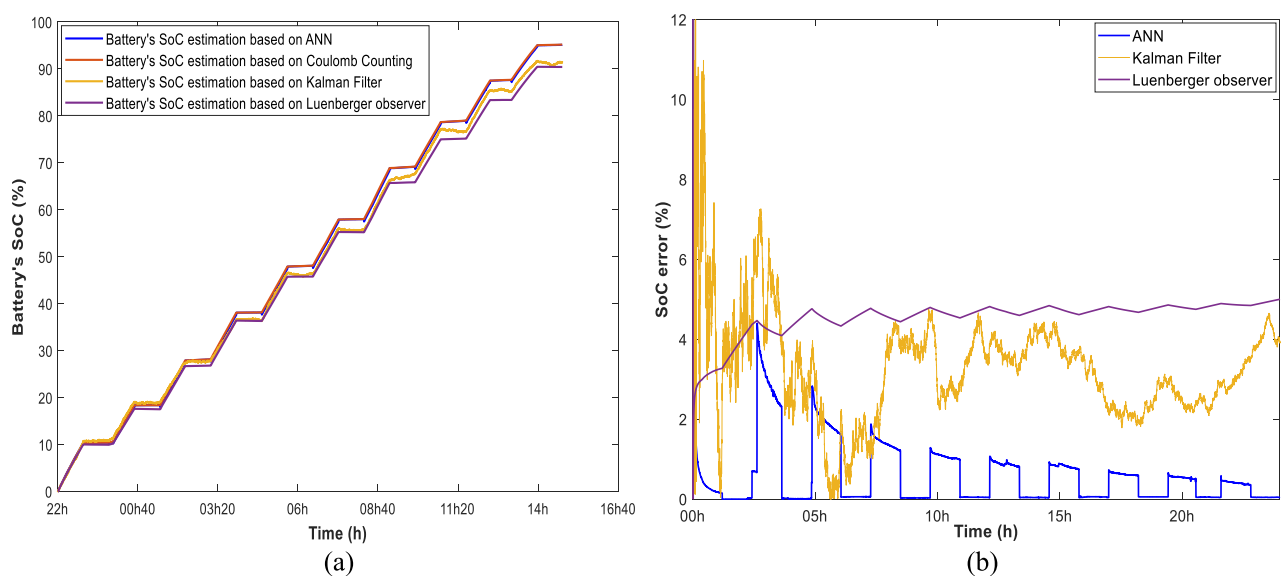


Fig. 19. (a) The battery's SoC, and (b) The SoC estimation error in the charging process.

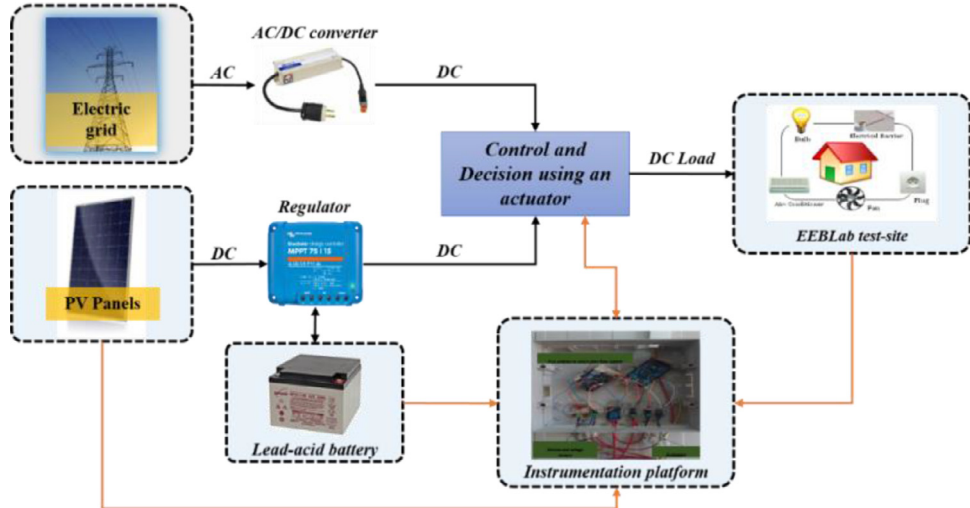


Fig. 20. The architecture of the MG system deployed in our test-bed.

Table 2
PV module's characteristics.

| Characteristics | Values |
|---|---------------------------------|
| Solar Cell number | 60 cells |
| Maximum Power At STC (P_{mpp}) | 265 W |
| Maximum Power Point Voltage (V_{mpp}) | 30.9 V |
| Maximum Power Current (I_{mpp}) | 8.58 A |
| Open Circuit Voltage (V_{oc}) | 38.3 V |
| Short Circuit Current (I_{sc}) | 8.98 A |
| Dimensions | 1640 × 992 × 40 mm ³ |
| Temperature coefficient of I_{sc} | 0.05%/°C |

order to extract the power in each branch of the MG system. The actuator is used to alter its position to the electric grid once the battery's SoC, which is estimated using the Coulomb Counting, achieves the threshold that is taken equal to 20% in this experiment. The platform is also composed of a Raspberry pi, which is used in order to collect the extracted data. Additionally, we have implemented the four SoC estimation methods, in the same Raspberry pi in order to estimate in real-time, using the collected data, the battery's SoC. The collected data as well as the estimated SoC are stored in our Big data platform for other purposes (e.g., visualization) [26]. The aim of this setup is to reveal the

behavior and performance of the MG system during 24 h and the accuracy of the battery model as well as the SoC estimation methods. Furthermore, we aim at comparing the four battery's SoC estimation methods in real-time. Therefore, an experiment and simulation of the system have been carried out during 24 h.

Fig. 21 presents the daily electricity consumption of our DC load, which is two ventilators with a maximum power of 24 W and a nominal voltage of 12 V, as well as the PV module production during 24 h. The load consumption as well as the PV production has been measured using a set of voltage and current sensors. As observed in Fig. 21(a), the DC load consumption, which is over 400 Wh, varies throughout the 24 h since it is controlled based on the CO₂ concentration in order to maintain a good indoor air quality while using less energy [65]. As for the PV production, which is depicted in Fig. 21(b), we can notice that before 7 AM and after 7 PM, there is no electricity production since there is no solar irradiation. On the other hand, the electricity production begins to increase after 7 AM until reaching 150 W at midday, and then decreases until 7 PM. We can also observe that the PV production during the afternoon is very low. This is caused by the fact that the sky was not clear, i.e., there was so many cloud, especially in the afternoon, and thus the PV production was less than usual.

Fig. 22 depicts the battery current as well as the experimental and

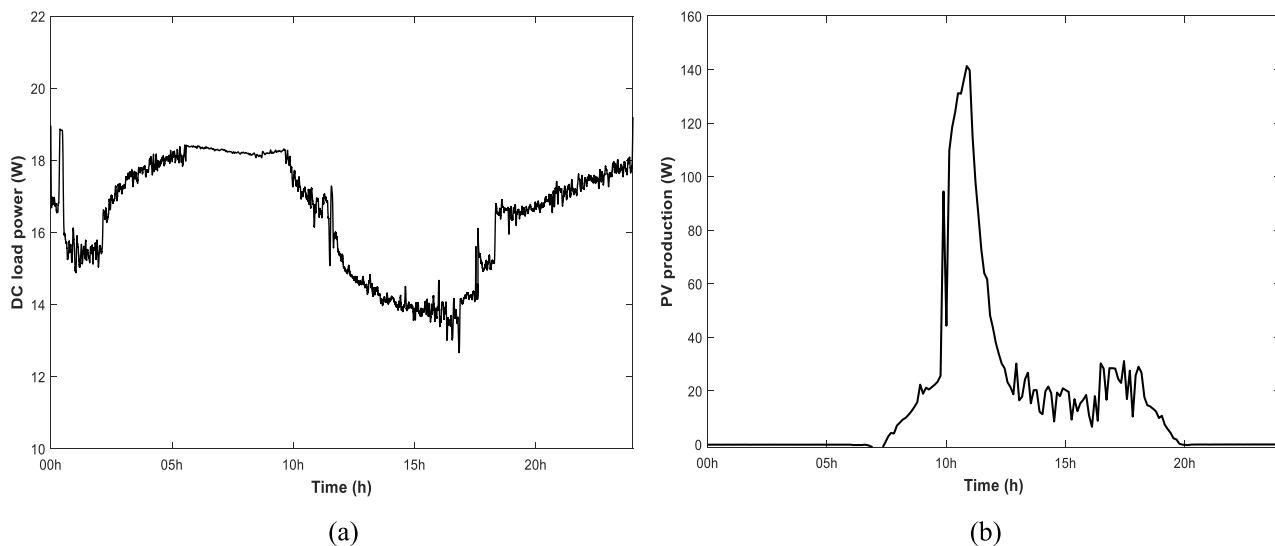


Fig. 21. (a) The DC load's daily electricity consumption, and (b) The PV production during 24 h.

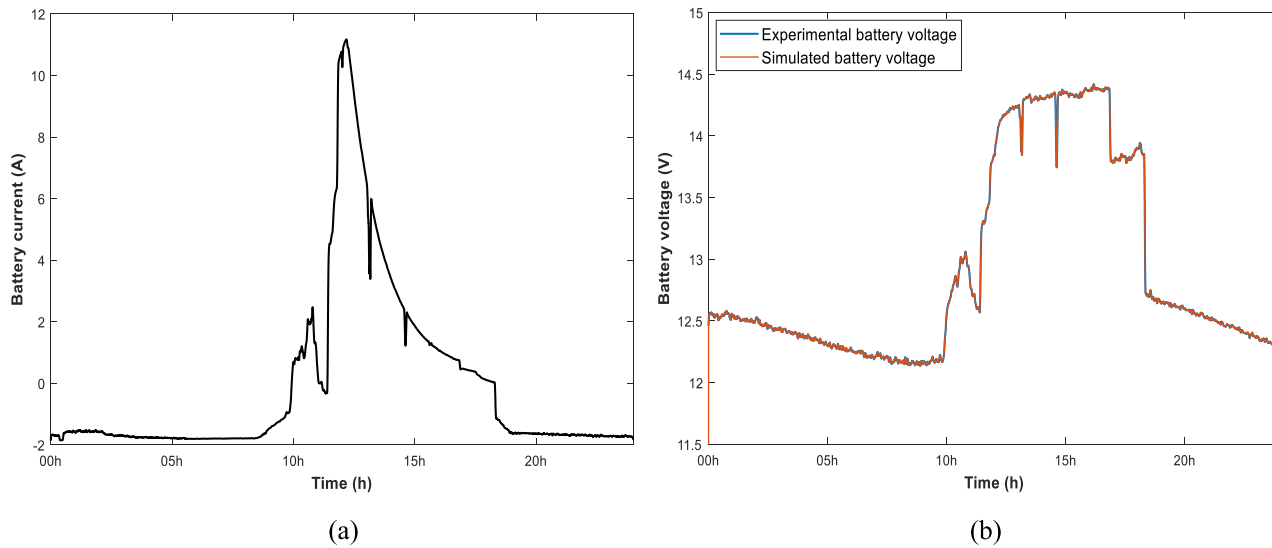


Fig. 22. (a) The battery current, and (b) The experimental and simulated battery voltage during 24 h.

simulated battery voltage during 24 h. As observed in Fig. 22(a), the battery discharges during the night (current negative) in order to supply the load with electricity while charges during the day (current positive) when the PV production is higher than the load consumption. As for the battery voltage, which is depicted in Fig. 22(b), it has similar behavior as the battery current. It decreases during the night and increases during the day until achieving its maximum voltage, which is almost 14.5 V. Regarding the simulated battery voltage, it has similar behavior and fits too well to the experimental one with a maximum error of about 1%, which does not reach the threshold. This slight error may be provoked by not taking into consideration the effect of temperature on the battery parameters in the model. These results lead us to conclude the accuracy of the battery model as well as the characterization methodology, especially when integrating them into an MG system.

Fig. 23 illustrates the estimated battery's SoC by the four methods as well as their errors when comparing them to the reference SoC (the one estimated by the Coulomb Counting method) during 24 h. This real-time estimation was performed in the Raspberry pi based on the extracted and collected data, which are the battery's current and voltage depicted in Fig. 22.

Table 3
SoC estimation errors of the three methods.

| Methods | Average error | Max error | RMSE |
|---------|---------------|-----------|--------|
| ANN | 0.122 | 0.434 | 0.1618 |
| KFCC | 1.088 | 2.823 | 1.27 |
| LO | 2.431 | 4.913 | 2.825 |

We can observe from Fig. 23(a) that the SoC estimated by the ANN, LO, and KFCC have similar behavior as the reference SoC with a slight error. In addition, we can notice that the SoC estimated by the ANN is the closest one to the reference SoC. Furthermore, Fig. 23(b) shows clearly that the SoC estimated by the ANN has the smallest error compared to the other methods. Also, we observe that the error of the SoC estimated by the ANN seeks to be as small as possible with time, and this is attributed to its learning capabilities. Besides, Table 3 presents the average error, the max error, and the RMSE, which are used to show the accuracy of the used methods when integrating them into an MG system. It can be clearly noticed that the average error, the max error, and the RMSE of the SoC estimated using the ANN method are smaller than those of the SoC estimated using the KFCC and the LO

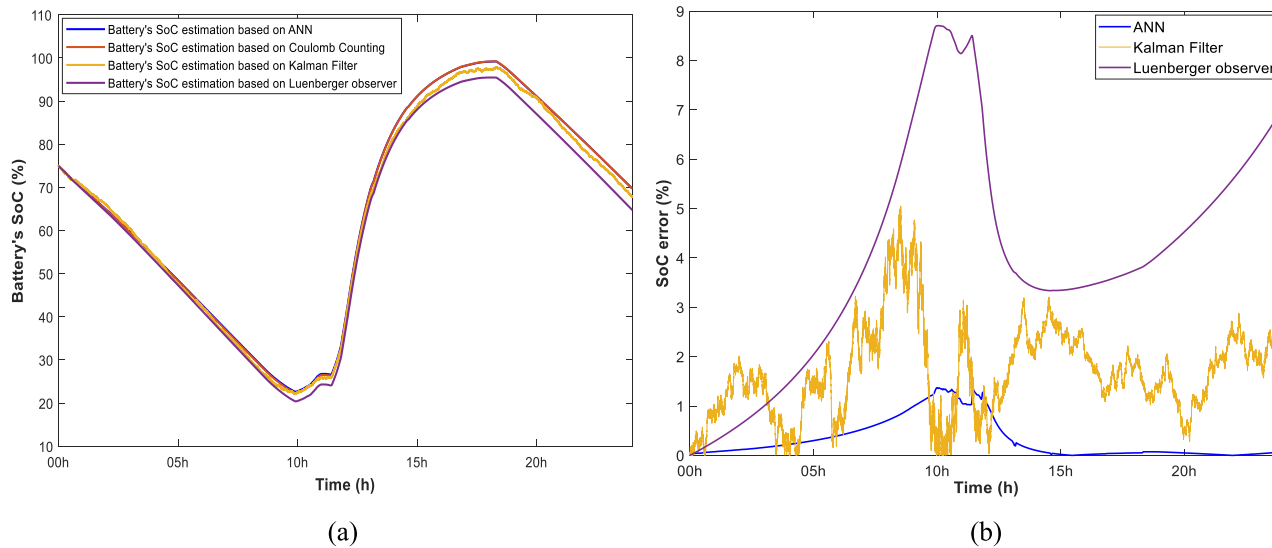


Fig. 23. (a) The battery's SoC, and (b) The SoC estimation error during 24 h.

methods. Therefore, the ANN has higher accuracy in real-time SoC estimation compared to the KFCC and LO methods. This can be caused by the fact that the KFCC and LO methods are based on the battery model and its identified parameters that depend also on the charge/discharge cycles, which make the errors of these two methods bigger than the error of the ANN method (i.e., their errors are bigger because of the accumulation of the errors of the battery model, the battery parameters identification and the SoC estimation).

5.4. Summary and discussions

From the results presented above, we can conclude that the proposed instrumentation platform has proved its effectiveness in both battery parameters identification and online SoC estimation for both isolated and integrated battery in MG system. Besides, we have assumed that the slight errors between the simulation and experimental results may be provoked by not taking into consideration the effect of temperature on the battery parameters in the model. These errors are too small, and this is attributed to the fact that the battery is placed in an air-conditioned room at 23 °C in both cases (i.e., isolated and integrated battery in MG system). In other words, since charging and discharging the battery takes several hours and the temperature of the room is approximately 23 °C all the time, thus the generated heat in the battery will be diffused by natural convection in the room, and therefore the battery temperature will not rise too much. However, the battery parameters are still affected by this rise in battery temperature. Therefore, the proposed instrumentation platform will be improved in our forthcoming work by incorporating temperature sensors in order to measure the battery temperature, and then use it to improve the battery characterization and modeling.

Besides, the proposed solution can be used with any other battery types. This is attributed to the fact that the instrumentation platform's components (e.g., sensors, data acquisition board) can be used to measure not only the characteristics of any battery types, but also the features of any other system (e.g., buildings' consumption, PV production) [63,66]. The RLS method, which has been used in this paper for online identification of battery's parameters, can also be used to characterize any other battery types as introduced by authors in [14]. Moreover, the 1RC model, which we have used for battery modeling, can be used in order to model any other battery types as presented by authors in [10,14,67,68]. Furthermore, the four SoC estimation methods, which are presented in this paper, can be used for estimating the SoC of any battery types [14,16]. Therefore, the proposed solution for battery characterization, modeling and SoC estimation is a generic solution that could be used with any battery types. On another note, one battery with 12 V as nominal voltage and 24 Ah as nominal capacity has been used in the studied MG system. However, for big MG systems that are used to provide buildings, for example, with electricity, many batteries, which are connected either in series or in parallel, are used. These battery packs have to be characterized, modeled and their SoC have to be estimated in order to protect them against the deep discharge and the overcharge. Also, the SoC can be used for controlling the MG system. For that, the proposed instrumentation platform can be used. Regarding the battery characterization and modeling, the instrumentation platform can be used to extract the characteristics (i.e., current and voltage) of one battery that will be used for identifying the battery parameters and validating its model, and then the model with the identified parameters will be used for all the other batteries if and only if all the batteries are of the same type and with the same state (e.g., new batteries). If not, each battery has to be characterized and modeled. Therefore, more current and voltage sensors will be needed.

Concerning the SoC estimation, many ways have been reviewed by authors in [40,69] in order to reach an accurate SoC estimation of battery packs. For instance, the simplest method is the "Big cell method". In this method the battery packs are considered as a big cell, and thus the voltage and current of the battery packs can be used to

estimate its SoC [40,69]. Despite its simplicity, it cannot ensure a high accuracy in estimating the battery packs' SoC. Also, establishing the relationship between OCV and SoC will need more SOC breakpoints in order to linearize the nonlinear parts of the OCV-SoC curve. In our case, the instrumentation platform can be used as it is in order to estimate the battery packs' SoC using the "Big cell method" and the four SoC methods. Another method, called "one by one calculation method", can be used for accurately estimating the battery packs' SoC [40,69]. In this method, the SoC of each battery is estimated, and then the SoC of the battery packs is computed. This method can ensure a high estimation accuracy. However, the complexity as well as the computation time increases. Contrary to the "Big cell method", the OCV-SoC curve of each battery will be extracted and used to estimate the battery's SoC using the model based methods (e.g., KF, LO). Regarding the proposed instrumentation platform, it can be used to estimate the battery packs' SoC using this method by adding more current and voltage sensors, which will be used for measuring the current and voltage of each battery. Besides, in the "screening process based method", the battery packs have to be composed of batteries with similar characteristics [69]. Then, the SoC of the battery packs is represented by the SoC of one battery due to the similarity of the batteries properties. This method gives a high accuracy in the beginning; however, the accuracy decreases with time (i.e., when the batteries start to degrade in a different ways). Besides, the proposed instrumentation platform can be used with this method without the addition of any sensors. These methods will be investigated in our forthcoming work for battery packs' SoC estimation in MG systems.

6. Conclusions and perspectives

In this work, a Lead-acid battery characterization, modeling and SoC estimation have been performed. In fact, an instrumentation platform, composed of recent and low cost sensing and actuating equipment, has been developed in order to identify the battery's parameters and then build its model. The simulation and experimental results have been compared, and their residuals have been found to be less than 5%, which show the efficiency of the battery characterization methodology and validate the battery model. This slight error could be provoked by not taking into account in the model the effect of temperature on the battery features. Then, a comparison between the four categories of battery's SoC estimation (i.e., CC, ANN, LO, and KFCC) in both charging and discharging processes has been performed in order to show and compare their performances. These algorithms have been afterwards included into our acquisition platform, which is connected to the same battery that has been already integrated into an MG system, in order to show and compare their accuracy for real-time battery's SoC estimation in MG systems. The results of the MG system showed a good agreement with the experimental results. As for the SoC estimation, the results showed that the SoC estimated by the ANN, LO, and KFCC have similar behavior as the reference SoC (CC), but the ANN has higher estimation accuracy. This can be explained by the fact that the KFCC and LO methods are based on the battery model and its identified parameters, which leads to an accumulation of errors. On the other hand, the ANN is learning, based on recent battery history and data, how to estimate and adapt the battery's SoC to the reference SoC, which makes this method more accurate. As perspectives, more simulations and experiments with other battery types will be conducted in order to prove that the proposed solution is a generic solution. Besides, we will focus on investigating the effect of the temperature on the battery model in order to improve it, and thus improving the accuracy of the SoC estimated by the KFCC and LO. Furthermore, we will focus on the forecasting of the battery's SoC in order to use it for controlling the MG system [70]. These methods are also under deployment and investigation in our electric vehicle platform for SoC estimation and prediction [71].

CRediT authorship contribution statement

Sofia Boulmrharj: Conceptualization, Methodology, Software, Formal analysis, Investigation, Data curation, Writing - original draft, Writing - review & editing, Visualization. **Radouane Ouladsine:** Conceptualization, Methodology, Software, Validation, Formal analysis, Data curation, Writing - review & editing. **Youssef NaitMalek:** Software, Formal analysis, Investigation, Data curation. **Mohamed Bakhouya:** Conceptualization, Methodology, Validation, Resources, Writing - review & editing, Project administration, Funding acquisition. **Khalid Zine-dine:** Project administration. **Mohammed Khaidar:** Methodology, Validation, Writing - review & editing, Supervision. **Mustapha Siniti:** Supervision.

Declaration of Competing Interest

The authors declare that they have no known competing financial interests or personal relationships that could have appeared to influence the work reported in this paper.

Acknowledgements

This work is supported by MIGRID project (grant 5-398, 2017–2019), which is funded by USAID under the PEER program.

References

- [1] S.O. Amrouche, D. Rekioua, T. Rekioua, S. Bacha, Overview of energy storage in renewable energy systems, Int. J. Hydrogen Energy 41 (2016) 20914–20927 Elsevier <https://doi.org/10.1016/j.ijhydene.2016.06.243>.
- [2] Q. Bajracharya, Dynamic modeling, monitoring and control of energy storage system, 2013.
- [3] S. Najafi-Shad, S.M. Barakati, A. Yazdani, An effective hybrid wind-photovoltaic system including battery energy storage with reducing control loops and omitting PV converter, J. Energy Storage 27 (2020), <https://doi.org/10.1016/j.est.2019.101088>.
- [4] M.R. Jongerden, B.R.H.M. Haverkort, *Battery modeling*, Enschede (2008).
- [5] S. Boulmrharj, Y. NaitMalek, A. El Mouatamid, R. Ouladsine, M. Bakhouya, M. Ouldoumoussa, K. Zine-dine, M. Khaidar, R. Abid, Towards a battery characterization methodology for performance evaluation of micro-grid systems, 2018 International Conference on Smart Energy Systems and Technologies (SEST), IEEE, 2018, pp. 1–6 <https://doi.org/10.1109/SEST.2018.8495829>.
- [6] D.O. Akinwale, R.K. Rayudu, Review of energy storage technologies for sustainable power networks, Sustain. Energy Technol. Assess. 8 (2014) 74–91 <https://doi.org/10.1016/j.seta.2014.07.004>.
- [7] U. Westerhoff, K. Kurbach, F. Lienesch, M. Kurrat, Analysis of lithium-ion battery models based on electrochemical impedance spectroscopy, Energy Technol. 4 (2016) 1620–1630 <https://doi.org/10.1002/ente.201600154>.
- [8] F.M. González-Longatt, *Circuit Based Battery Models: a Review*, In Congreso Iberoamericano de estudiantes De Ingeniería Electrica, Gibelet, 2006.
- [9] O. Tremblay, L.A. Dessaint, Experimental validation of a battery dynamic model for EV applications, World Electr. Veh. J. 3 (2009) 289–298 <https://doi.org/10.3390/wevj3020289>.
- [10] S.J. Lee, J.H. Kim, J.M. Lee, B.H. Cho, The state and parameter estimation of an Li-ion battery using a new OCV-SOC concept, 2007 IEEE Power Electronics Specialists Conference, 2007, pp. 2799–2803 <https://doi.org/10.1109/PESC.2007.4342462>.
- [11] P. Mauracher, E. Karden, Dynamic modelling of lead/acid batteries using impedance spectroscopy for parameter identification, J. Power Sources 67 (1997) 69–84 [https://doi.org/10.1016/S0378-7753\(97\)02498-1](https://doi.org/10.1016/S0378-7753(97)02498-1).
- [12] G.L. Plett, Extended Kalman filtering for battery management systems of LiPB-based HEV battery packs: part 3. State and parameter estimation, J. Power Sources 134 (2004) 277–292 <https://doi.org/10.1016/j.jpowsour.2004.02.033>.
- [13] Dd-I. Stroe, M. Swierczynski, A.-I. Stroe, S. Knudsen Kær, Generalized characterization methodology for performance modelling of lithium-ion batteries, Batteries 2 (2016), <https://doi.org/10.3390/batteries2040037>.
- [14] B. Xia, Z. Lao, R. Zhang, Y. Tian, G. Chen, Z. Sun, W. Wang, W. Sun, Y. Lai, M. Wang, H. Wang, Online parameter identification and state of charge estimation of lithium-ion batteries based on forgetting factor recursive least squares and nonlinear Kalman filter, Energies 11 (2018), <https://doi.org/10.3390/en11010003>.
- [15] W.Y. Chang, The state of charge estimating methods for battery: a review, ISRN Appl. Math. (2013), <http://dx.doi.org/10.1155/2013/953792>.
- [16] J.P. Rivera-Barrera, N. Muñoz-Galeano, H.O. Sarmiento-Maldonado, SoC estimation for lithium-ion batteries: review and future challenges, Electronics 6 (2017), <https://doi.org/10.3390/electronics6040102>.
- [17] X. Hu, F. Feng, K. Liu, L. Zhang, J. Xie, B. Liu, State estimation for advanced battery management: key challenges and future trends, Renew. Sustain. Energy Rev. 114 (2019), <https://doi.org/10.1016/j.rser.2019.109334>.
- [18] M.A. Hannan, M.H. Lipu, A. Hussain, A. Mohamed, A review of lithium-ion battery state of charge estimation and management system in electric vehicle applications: challenges and recommendations, Renew. Sustain. Energy Rev. 78 (2017) 834–854 <https://doi.org/10.1016/j.rser.2017.05.001>.
- [19] X. Hu, H. Yuan, C. Zou, Z. Li, L. Zhang, Co-estimation of state of charge and state of health for lithium-ion batteries based on fractional-order calculus, IEEE Trans. Veh. Technol. 67 (2018) 10319–10329 <https://doi.org/10.1109/TVT.2018.2865664>.
- [20] X. Hu, H. Jiang, F. Feng, B. Liu, An enhanced multi-state estimation hierarchy for advanced lithium-ion battery management, Appl. Energy 257 (2020), <https://doi.org/10.1016/j.apenergy.2019.114019>.
- [21] C. Zhang, J. Jiang, L. Zhang, S. Liu, L. Wang, P. Chiang, A generalized SOC-OCV model for lithium-ion batteries and the SOC estimation for LNMC battery, Energies 9 (2016), <https://doi.org/10.3390/en9110900>.
- [22] Z. Zeng, J. Tian, D. Li, Y. Tian, An online state of charge estimation algorithm for Lithium-ion batteries using an improved adaptive cubature Kalman filter, Energies 11 (2018), <https://doi.org/10.3390/en11010059>.
- [23] A. Vasebi, M. Partovibakhsh, S.M. Taghi Bathaei, A novel combined battery model for state-of-charge estimation in lead-acid batteries based on extended Kalman filter for hybrid electric vehicle applications, J. Power Sources 174 (2007) 30–40 Elsevier <https://doi.org/10.1016/j.jpowsour.2007.04.011>.
- [24] M. Charkhgard, M. Farrokhi, State-of-charge estimation for lithium-ion batteries using neural networks and EKF, IEEE Trans. Ind. Electron. 57 (2010) 4178–4187 <https://doi.org/10.1109/TIE.2010.2043035>.
- [25] Z. Chen, S. Qui, M. Abul Masrur, Y.L. Murphrey, Battery State of Charge estimation based on a combined model of extended kalman filter and neural networks, The 2011 International Joint Conference on Neural Networks, IEEE, 2011, pp. 2156–2163 <https://doi.org/10.1109/IJCNN.2011.6033495>.
- [26] M. Bakhouya, Y. NaitMalek, A. Elmouatamid, F. Lachhab, A. Berouine, S. Boulmrharj, R. Ouladsine, V. Felix, K. Zine-dine, M. Khaidar, N. Elkamoune, Towards a data-driven platform using IoT and Big Data technologies for energy efficient buildings, 2017 3rd International Conference of Cloud Computing Technologies and Applications (CloudTech), 2017 <https://doi.org/10.1109/CloudTech.2017.8284744>.
- [27] S. Boulmrharj, R. Rabeh, V. Felix, R. Ouladsine, M. Bakhouya, K. Zine-dine, M. Khaidar, M. Siniti, R. Abid, Modeling and dimensioning of grid-connected photovoltaic systems, 2017 International Renewable and Sustainable Energy Conference (IRSEC), IEEE, 2017, <https://doi.org/10.1109/IRSEC.2017.8477392>.
- [28] Y.N.M.S.Boulmrharj, A. El Mouatamid, M. Bakhouya, R. Ouladsine, K. Zine-Dine, M. Khaidar, M. Siniti, Battery characterization and dimensioning approaches for micro-grid systems, Energies 12 (2019), <https://doi.org/10.3390/en12071305>.
- [29] M. Elibrahimi, A. Elmouatamid, M. Bakhouya, K. Feddi, R. Ouladsine, Performance evaluation of fixed and sun tracking photovoltaic systems, 2018 6th International Renewable and Sustainable Energy Conference (IRSEC), IEEE, 2018 December <https://doi.org/10.1109/IRSEC.2018.8702932>.
- [30] A. El Mouatamid, Y. Nait Malek, R. Ouladsine, M. Bakhouya, N. ElKamoun, K. Zine-Dine, M. Khaidar, R. Abid, Towards a demand/response control approach for micro-grid systems, 2018 5th International Conference on Control, Decision and Information Technologies (CoDIT), IEEE, 2018, pp. 984–988 <https://doi.org/10.1109/CoDIT.2018.8394951>.
- [31] M. Luzi, M. Paschero, A. Rossini, A. Rizzi, F.M.F. Mascioli, Comparison between two nonlinear kalman filters for reliable SoC estimation on a prototypal bms, IECON 2016-42nd Annual Conference of the IEEE Industrial Electronics Society, IEEE, 2016, pp. 5501–5506 October <https://doi.org/10.1109/IECON.2016.7794054>.
- [32] B. Belvedere, M. Bianchi, A. Borghetti, C.A. Nucci, M. Paolone, A. Peretto, A microcontroller-based power management system for standalone microgrids with hybrid power supply, IEEE Trans. Sustain. Energy 3 (2012) 422–431 <https://doi.org/10.1109/TSTE.2012.2188654>.
- [33] S. Blaifi, S. Moulahoum, I. Colak, W. Merrouche, Monitoring and enhanced dynamic modeling of battery by genetic algorithm using LabVIEW applied in photovoltaic system, Electr. Eng. 100 (2018) 1021–1038 <https://doi.org/10.1007/s00202-017-0567-6>.
- [34] D. Arcos-Aviles, J. Pascual, L. Marroyo, P. Sanchis, F. Guinjoan, Fuzzy logic-based energy management system design for residential grid-connected microgrids, IEEE Trans. Smart Grid 9 (2016) 530–543 <https://doi.org/10.1109/TSG.2016.2555245>.
- [35] Y. Cheddadi, A. Gaga, F. Errahimi, N.E. Sbai, Design of an energy management system for an autonomous hybrid micro-grid based on Labview IDE, 2015 3rd International Renewable and Sustainable Energy Conference (IRSEC), IEEE, 2015 December <https://doi.org/10.1109/IRSEC.2015.7454965>.
- [36] K.G.H. Mangunkusumo, K.L. Lian, P. Aditya, Y.R. Chang, Y.D. Lee, Y.H. Ho, A battery management system for a small microgrid system, 2014 International Conference on Intelligent Green Building and Smart Grid (IGBSG), IEEE, 2014 April <https://doi.org/10.1109/IGBSG.2014.6835277>.
- [37] A. Berrueta, I. San Martín, P. Sanchis, A. Ursúa, Comparison of State-of-Charge estimation methods for stationary Lithium-ion batteries, IECON 2016-42nd Annual Conference of the IEEE Industrial Electronics Society, IEEE, 2016, pp. 2010–2015 October <https://doi.org/10.1109/IECON.2016.7794094>.
- [38] H. Hinz, Comparison of lithium-ion battery models for simulating storage systems in distributed power generation, Inventions 4 (2019), <https://doi.org/10.3390/inventions4030041>.
- [39] A. Hentunen, T. Lehmuspelto, J. Suomela, Time-domain parameter extraction method for Thévenin-equivalent circuit battery models, IEEE Trans. Energy Convers. 29 (2014) 558–566 <https://doi.org/10.1109/TEC.2014.2318205>.
- [40] G.S. Misirys, D.I. Doukas, T.A. Papadopoulos, D.P. Labridis, V.G. Agelidis, State-of-charge estimation for li-ion batteries: a more accurate hybrid approach, IEEE Trans. Energy Convers. 34 (2018) 109–119 <https://doi.org/10.1109/TEC.2018.2861994>.
- [41] S. Barsali, M. Ceraolo, Dynamical models of lead-acid batteries: implementation

- issues, *IEEE Trans. Energy Convers.* 17 (2002) 16–23 <https://doi.org/10.1109/60.986432>.
- [42] A. Fotouhi, D.J. Auger, K. Propp, S. Longo, Accuracy versus simplicity in online battery model identification, *IEEE Trans. Syst. Man Cybern.* 48 (2016) 195–206 <https://doi.org/10.1109/TSMC.2016.2599281>.
- [43] X. Hu, S. Li, H. Peng, A comparative study of equivalent circuit models for Li-ion batteries, *J. Power Sources* 198 (2012) 359–367 <https://doi.org/10.1016/j.jpowsour.2011.10.013>.
- [44] H.S. Ramadan, M. Becherif, F. Claude, Extended kalman filter for accurate state of charge estimation of lithium-based batteries: a comparative analysis, *Int. J. Hydrogen Energy* 42 (2017) 29033–29046 <https://doi.org/10.1016/j.ijhydene.2017.07.219>.
- [45] I. Baccouche, B.M. Jemmali, N. Omar, N. Essoukri Ben Amara, Improved OCV model of a Li-Ion NMC Battery for Online SOC estimation using the extended Kalman filter, *Energies* 10 (2017), <https://doi.org/10.3390/en10060764>.
- [46] M. Daoud, N. Omar, B. Verbrugge, P. Van Den Bossche, J. Van Mierlo, Battery models parameter estimation based on MATLAB/Simulink®, Proceedings of the 25th Electric Vehicle Symposium (EVS-25), Shenzhen, China, 59 2010, November.
- [47] A. Vasebi, M. Partovibakhsh, S.M. Taghi Bathaei, Predicting state of charge of lead-acid batteries for hybrid electric vehicles by extended Kalman filter, *Energy Convers. Manag.* 49 (2008) 75–82 Elsevier <https://doi.org/10.1016/j.enconman.2007.05.017>.
- [48] L. Zhang, M. Dou, J. Gao, Parameter Identification Method for Lithium-Ion Battery Model with Multi Frequency AC Signal Injection, *Rev. Téc. Ing. Univ. Zulia* 39(2016) 221–227.
- [49] D. Haifeng, W. Xuezhe, S. Zechang, State and parameter estimation of a HEV Li-ion battery pack using adaptive Kalman filter with a new SOC-OCV concept, 2009 International Conference on Measuring Technology and Mechatronics Automation, 2 IEEE, 2009, pp. 375–380 <https://doi.org/10.1109/ICMTMA.2009.333>.
- [50] D.N. How, M.A. Hannan, M.H. Lipu, P.J. Ker, State of charge estimation for lithium-ion batteries using model-based and data-driven methods: a review, *IEEE Access* 7 (2019) 136116–136136 <https://doi.org/10.1109/ACCESS.2019.2942213>.
- [51] P. Shrivastava, T.K. Soon, M.Y.I.B. Idris, S. Mekhilef, Overview of model-based online state-of-charge estimation using Kalman filter family for lithium-ion batteries, *Renew. Sustain. Energy Rev.* 113 (2019), <https://doi.org/10.1016/j.rser.2019.06.040>.
- [52] M.U. Ali, A. Zafar, S.H. Nengroo, S. Hussain, M. Junaid Alvi, H.J. Kim, Towards a smarter battery management system for electric vehicle applications: a critical review of lithium-ion battery state of charge estimation, *Energies* 12 (2019), <https://doi.org/10.3390/en12030446>.
- [53] A.M.S.M.H.S. Attanayaka, J.P. Karunadasa, K.T.M.U. Hemapala, Estimation of state of charge for lithium-ion batteries-a review, *AIMS Energy* 7 (2019), <https://doi.org/10.3934/energy.2019.2.186>.
- [54] S. Tong, J.H. Lacap, J.W. Park, Battery state of charge estimation using a load-classifying neural network, *J. Energy Storage* 7 (2016) 236–243 <https://doi.org/10.1016/j.est.2016.07.002>.
- [55] M.A. Awadallah, B. Venkatesh, Accuracy improvement of SOC estimation in lithium-ion batteries, *Journal of Energy Storage* 6 (2016) 95–104 <https://doi.org/10.1016/j.est.2016.03.003>.
- [56] N. Watrin, B. Blunier, A. Miraoui, Review of adaptive systems for lithium batteries state-of-charge and state-of-health estimation, 2012 IEEE Transportation Electrification Conference and Expo (ITEC), 2012 <https://doi.org/10.1109/ITEC.2012.6243437>.
- [57] I.-H. Li, W.-Y. Wang, S.-F. Su, Y.-S. Lee, A merged fuzzy neural network and its applications in battery state-of-charge estimation, *IEEE Trans. Energy Convers.* 22 (2007) 697–708 <https://doi.org/10.1109/TEC.2007.895457>.
- [58] X. Hu, L. Xu, X. Lin, M. Pecht, Battery lifetime prognostics, *Joule* 4 (2020) 310–346 <https://doi.org/10.1016/j.joule.2019.11.018>.
- [59] X. Hu, F. Sun, Y. Zou, Estimation of state of charge of a lithium-ion battery pack for electric vehicles using an adaptive Luenberger observer, *Energies* 3 (2010) 1586–1603 <https://doi.org/10.3390/en3091586>.
- [60] F. Codecà, S.M. Savaresi, G. Rizzoni, On battery state of charge estimation: a new mixed algorithm, 2008 IEEE International Conference on Control Applications, IEEE, 2008, pp. 102–107. <https://doi.org/10.1109/CCA.2008.4629635>
- [61] W.Y. Chang, Estimation of the state of charge for a LiFP battery using a hybrid method that combines a RBF neural network, an OLS algorithm and AGA, *Int. J. Electr. Power Energy Syst.* 53 (2013) 603–611 <https://doi.org/10.1016/j.ijepes.2013.05.038>.
- [62] J. Wang, B. Cao, Q. Chen, F. Wang, Combined state of charge estimator for electric vehicle battery pack, *Control Eng. Pract.* 15 (2007) 1569–1576 <https://doi.org/10.1016/j.conengprac.2007.03.004>.
- [63] R. Khwanrit, S. Kittipiyakul, J. Kudtonagngam, H. Fujita, Accuracy comparison of present low-cost current sensors for building energy monitoring, 2018 International Conference on Embedded Systems and Intelligent Technology & International Conference on Information and Communication Technology for Embedded Systems (ICESIT-ICICTES), IEEE, May 2018, <https://doi.org/10.1109/ICESIT-ICICTES.2018.8442066>.
- [64] H. Zhang, M. Zhou, X. Lan, State of charge estimation algorithm for unmanned aerial vehicle power-type lithium battery packs based on the extended Kalman filter, *Energies* 12 (2019), <https://doi.org/10.3390/en12203960>.
- [65] H. Elkhokhi, Y. NaitMalek, M. Bakhouya, A. Berouine, A. Kharbouch, F. Lachhab, M. Hanifi, D. El Ouadghiri, M. Essaaidi, A platform architecture for occupancy detection using stream processing and machine learning approaches, *Concurr. Comput.* (2019), <https://doi.org/10.1002/cpe.5651>.
- [66] A. Jamaluddin, L. Sihombing, A. Supriyanto, A. Purwanto, M. Nizam, Design real time battery monitoring system using labview interface for arduino (lifa), 2013 Joint International Conference on Rural Information & Communication Technology and Electric-Vehicle Technology (rICT & ICeV-T), 2013 <https://doi.org/10.1109/rICT-ICeVT.2013.6741525>.
- [67] K.C. Bae, S.C. Choi, J.H. Kim, C.Y. Won, Y.C. Jung, LiFePO₄ dynamic battery modeling for battery simulator, 2014 IEEE International Conference on Industrial Technology (ICIT), IEEE, 2014, pp. 354–358 <https://doi.org/10.1109/ICIT.2014.6894892>.
- [68] H. He, R. Xiong, J. Fan, Evaluation of lithium-ion battery equivalent circuit models for state of charge estimation by an experimental approach, *Energies* 4 (2011) 582–598 <https://doi.org/10.3390/en4040582>.
- [69] R. Xiong, J. Cao, Q. Yu, H. He, F. Sun, Critical review on the battery state of charge estimation methods for electric vehicles, *IEEE Access* 6 (2017) 1832–1843 <https://doi.org/10.1109/ACCESS.2017.2780258>.
- [70] Y. Naitmalek, M. Najib, M. Bakhouya, M. Essaaidi, Forecasting the state-of-charge of batteries in micro-grid systems, 2019 4th World Conference on Complex Systems (WCCS), IEEE, 2019, <https://doi.org/10.1109/ICoCS.2019.8930731>.
- [71] Y. Naitmalek, M. Najib, M. Bakhouya, M. Essaaidi, On the use of machine learning for state-of- charge forecasting in electric vehicles, 2019 IEEE International Smart Cities Conference (ISC2), IEEE, 2019In press.